Remote Sensing of Environment xxx (xxxx) xxx

Contents lists available at ScienceDirect

Remote Sensing of Environment

journal homepage: www.elsevier.com/locate/rse

Monitoring road development in Congo Basin forests with multi-sensor satellite imagery and deep learning

Bart Slagter [a,*], Kurt Fesenmyer [b], Matthew Hethcoat [c], Ethan Belair [b], Peter Ellis [b], Fritz Kleinschroth [d,e], Marielos Peña-Claros [f], Martin Herold [a,g], Johannes Reiche [a]

[a] Laboratory of Geo-Information Science and Remote Sensing, Wageningen University & Research, the Netherlands
[b] The Nature Conservancy, Arlington, Virginia, United States of America
[c] Northern Forestry Centre, Canadian Forest Service, Natural Resources Canada, Edmonton, Canada
[d] Institute of Environmental Planning, Leibniz University Hannover, Germany
[e] Ecosystem Management, Department of Environmental Systems Science, ETH Zurich, Switzerland
[f] Forest Ecology and Forest Management Group, Wageningen University & Research, the Netherlands
[g] Helmholtz GFZ German Research Centre for Geosciences, Remote Sensing and Geoinformatics, Potsdam, Germany

ARTICLE INFO

Edited by Marie Weiss

Keywords:
Artificial intelligence
Central Africa
Deforestation
Forest degradation
Logging
Roads
Sentinel-1
Sentinel-2

ABSTRACT

Road development has affected many remote tropical forests around the world and has accelerated human-induced deforestation, forest degradation and biodiversity loss. The development of roads in tropical forests is largely driven by industrial selective logging, which can provide a sustainable source of revenue for developing countries while avoiding more detrimental forms of forest degradation or deforestation. Understanding the dynamics and impacts of road development is challenging, because road inventories in remote tropical forests have been largely incomplete or outdated. In this study, we present novel remote sensing-based methods for automated monitoring of road development and apply them across the Congo Basin forest region, an area characterized by increasing road development rates driven by logging activities. We trained a deep learning model with Sentinel-1 and -2 satellite imagery to map road development on a monthly basis at 10 m spatial scale, leveraging the complementary value of radar and optical imagery. Applying the model across the Congo Basin forest, we present a vectorized map of road development from January 2019 until December 2022, demonstrating an F1-score of 0.909, a false detection rate of 4.2% and a missed detection rate of 14.9%. In total, we mapped 35,944 km of road development in the Congo Basin forest during the four years, with at least 78% apparently related to logging activities, mainly located in the western part of the region. We estimate that 30% of the detected road openings were previously abandoned logging roads that were reopened. In addition, 23% of detected road development was located in areas considered to be intact forest landscapes. The road monitoring methods demonstrated in this study can facilitate several crucial forest management and conservation objectives in the tropics, such as assessing ecological and climate impacts related to selective logging, monitoring illegal or unsustainable activities, and providing a basis for improved understanding and evaluation of human impacts on forests at large scale. More information, including a full overview of the Congo Basin forest road map, can be found at: https://wur.eu/forest-roads.

1. Introduction

In recent decades, extensive road development has facilitated access to many remote and intact tropical forests (Engert et al., 2024; Gaveau et al., 2014; Kleinschroth et al., 2019b). This raises many concerns, because road development in tropical forests has shown to accelerate human-induced deforestation, forest degradation and biodiversity loss (Asner et al., 2006; Barber et al., 2014; Engert et al., 2024; Gaveau et al., 2021; Ibisch et al., 2016; Kleinschroth et al., 2019b; Laurance et al., 2009, 2014).

The Congo Basin forest region represents the second largest tropical forest in the world and has experienced increasing rates of road

* Corresponding author at: Laboratory of Geo-Information Science and Remote Sensing, Wageningen University & Research, Droevendaalsesteeg 3, 6708 PB Wageningen, the Netherlands.
E-mail address: bart.slagter@wur.nl (B. Slagter).

https://doi.org/10.1016/j.rse.2024.114380
Received 13 March 2024; Received in revised form 3 July 2024; Accepted 19 August 2024

development (Kleinschroth et al., 2019b), primarily driven by the forestry sector to access remote forests for selective logging activities. Commercial logging concessions are an important economic opportunity for the developing countries of the Congo Basin forest, contributing substantially to the regional economy (African Natural Resources Centre, 2021). In general, selective logging in sustainably managed forests can provide profitable timber harvests, while maintaining forest conservation values, and is commonly favored over more destructive land uses, such as complete forest clearing for large-scale agricultural activities (Edwards et al., 2014; Gibson et al., 2011; Putz et al., 2012). While it is notable that the Congo Basin forest generally experiences low logging intensities compared to more intensively managed forests in Southeast Asia and South America (Dupuis et al., 2023; Umunay et al., 2019), the rapidly expanding logging road development in the region has drawn serious concerns for forest ecosystems, carbon stocks and biodiversity (Kleinschroth et al., 2019b).

The impacts of logging roads differ from permanent roads (Kleinschroth et al., 2019b; Kleinschroth and Healey, 2017). Logging roads are commonly unpaved, only temporarily used, and left to revegetate after a logging operation (Kleinschroth et al., 2015). Despite being transient, they are associated with multiple ecological and climate impacts. Primarily, the clearing of forest corridors for road development is the largest source of carbon emissions associated with selective logging (Ellis et al., 2019). Road openings also lead to soil erosion and compaction, edge effects, habitat fragmentation and increased risks of forest fires (Laurance et al., 2009). Secondary, more detrimental impacts may occur when abandoned logging roads remain accessible to the public and facilitate unauthorized activities in remote forests, such as agricultural colonization, mining, poaching or artisanal logging (Kleinschroth and Healey, 2017; Laurance et al., 2009). When old logging roads are eventually adopted for permanent use, extensive deforestation can occur in their surroundings (Kleinschroth and Healey, 2017). These secondary impacts are particularly concerning because, in recent decades, many logging road networks have been developed in areas with no previous indications of human activities, identified as intact forest landscapes (IFL) (Potapov et al., 2008, 2017).

Given the substantial impacts of proliferating road networks in tropical forests, efficient large-scale monitoring of road development serves multiple crucial purposes. First, detailed road maps can assist in the assessment of ecological impacts and carbon emissions associated with selective logging activities (Pearson et al., 2014; Umunay et al., 2019). Furthermore, timely road monitoring can aid in rapid law enforcement against illegally opened roads, or combating the unauthorized activities in abandoned logging road networks. (Kleinschroth and Healey, 2017; Laurance et al., 2009). Finally, at a larger scale, wall-to-wall road maps can be used as a basis for conservation strategies, evaluating terrestrial human footprints or forest intactness (Potapov et al., 2008, 2017; Riggio et al., 2020; Venter et al., 2016).

Although many attempts have been done to map roads in tropical forests, current road inventories are largely incomplete or outdated (Barber et al., 2014; Engert et al., 2024; Sloan et al., 2018). Road mapping efforts have historically relied on labor-intensive manual digitization (e.g., Brandão and Souza, 2006; Engert et al., 2024; Gaveau et al., 2014, 2021; Kleinschroth et al., 2019b; Laporte et al., 2007), commonly based on medium resolution optical satellite imagery (e.g., 30 m resolution Landsat data) with limited multitemporal coverage due to cloud cover. Consequently, narrow or rapidly overgrowing road segments are commonly missed in road inventories in tropical forests.

An automated road mapping system based on artificial intelligence is currently one of the most urgent conservation needs for tropical forests (Engert et al., 2024). In recent years, the emergence of deep learning techniques has advanced the automated extraction of road maps from satellite imagery (Abdollahi et al., 2020; Chen et al., 2022; Lian et al., 2020), mainly for urban regions. Deep learning-based road mapping in tropical forests specifically has recently been explored with promising results (Botelho et al., 2022; Sloan et al., 2024), but still poses specific challenges. For example, the canopy above logging roads can quickly close after a timber harvest, making them only temporarily visible in satellite imagery (Fig. 1). This is particularly problematic for road detections in the densely cloud-covered Congo Basin forest, where many transient road segments can go unnoticed. Therefore, it is of high importance that road maps are frequently updated and thus based on high spatiotemporal resolution satellite imagery.

Since the launch of the Sentinel-1 and Sentinel-2 satellites in 2014 and 2015 respectively, high spatiotemporal resolution satellite imagery (10-20 m resolution) is now openly available (Drusch et al., 2012; Torres et al., 2012). This has led to an improved near real-time monitoring of small-scale forest changes (e.g., Doblas et al., 2022; Mermoz et al., 2021; Pickens et al., 2020a; Reiche et al., 2021), compared to previous efforts based on medium resolution (30-50 m) satellite data (e.g., Diniz et al., 2015; Hansen et al., 2016; Vargas et al., 2019; Watanabe et al., 2021). In particular, the cloud-penetrating radar sensors aboard Sentinel-1 offer a major advantage for near real-time forest disturbance alerting systems in the tropics. Yet, current systems are all tailored for generic forest disturbance detection and do not present a thematic distinction between roads and other types of forest changes, such as agriculture-driven clearings or natural disturbances. While methods have been presented to attribute specific drivers to detected disturbances, including roads (Slagter et al., 2023), the underlying disturbance alerting systems have a limited capacity to detect road development in general, because these are narrow and small-scale changes that are often not or only partly detected. Even with the use of higher resolution imagery, road development remains among the most challenging disturbance types to distinguish (Dalagnol et al., 2023) and may require specific deep learning-based detection methods.

In this paper, we present automated remote sensing-based methods to monitor road development in tropical forests. We demonstrate the use of deep learning techniques applied to Sentinel-1 and -2 imagery for accurate and timely road detections. We produce and evaluate a vectorized road development map covering four years (2019-2022) for the entire Congo Basin forest.

2. Methodology

The methodology overview of this study is presented in Fig. 2. First, based on Sentinel-1 and -2 imagery and a collected road reference dataset, we trained a convolutional neural network (CNN) tailored for detecting newly opened roads. Then, this model was applied across the entire Congo Basin forest region to map road development on a monthly basis between 2019 and 2022. To understand how road detection capacities varied per sensor and ecoregion, we tested the sensor- and ecoregion-specific model performance based on a held-out subset of reference data. The accuracy of the wall-to-wall Congo Basin forest road map was separately assessed based on a stratified random sample. Lastly, we combined our road map with complementary geospatial datasets to analyze different road opening types, practices and locations in the Congo Basin forest.

2.1. Study area

We defined our study area as the tropical moist forests within the six Central African countries Cameroon, Central African Republic, the Democratic Republic of the Congo (DRC), Equatorial Guinea, Gabon, and the Republic of the Congo (RoC), between 6°N and 6°S (Fig. 3). All areas defined as primary humid tropical forest (based on Turubanova et al., 2018) or having >75% tree cover (based on Hansen et al., 2013) were included. From this forest baseline, we excluded areas with forest loss until 2018 (based on Hansen et al., 2013) and remaining small forest fragments <10 ha.

We defined four separate ecoregions for the Congo Basin forest (Northwest, Southwest, Central and East) based on diurnal irradiance regimes mapped by Philippon et al. (2019) (Fig. 3). These regimes are

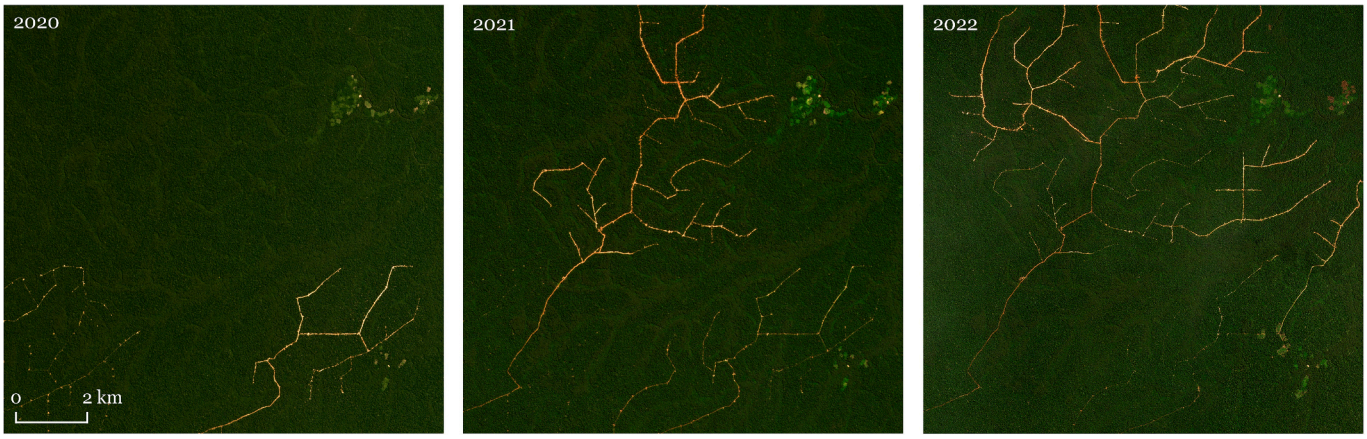

Fig. 1. High-resolution Planet imagery showing logging road development and rapid canopy regrowth at older roads in a logging concession in the Democratic Republic of the Congo (central coordinate: 1.14°N, 22.70°E).

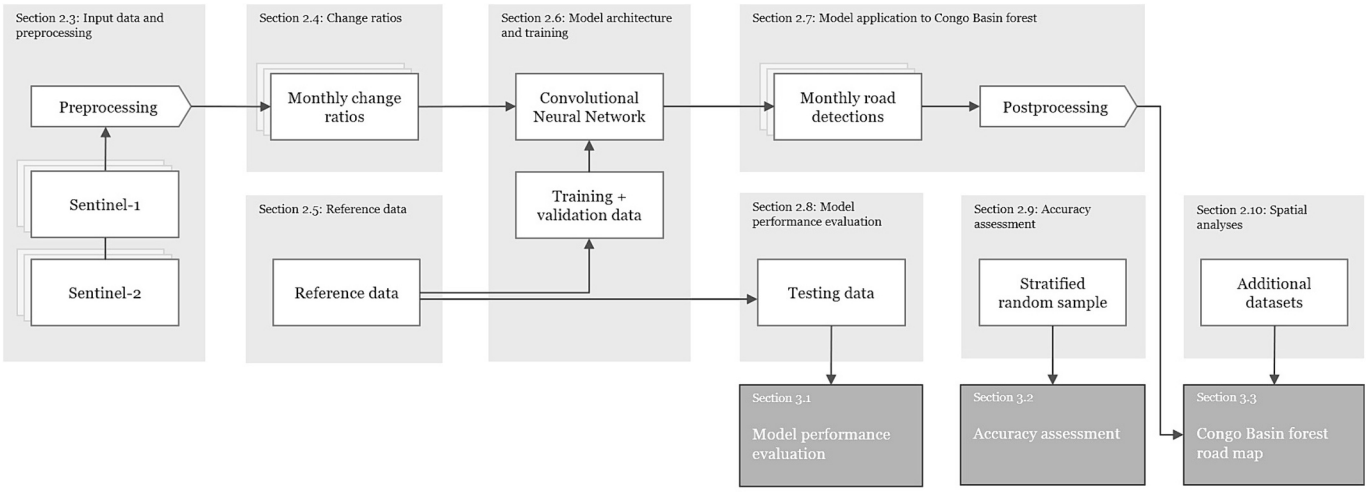

Fig. 2. Methodology overview of this study to monitor road development in the Congo Basin forest.

derived from seasonal patterns of cloud cover and precipitation, and have been linked to differences in regional forest structure and composition. For example, the Northwest and Southwest ecoregions are characterized by higher cloud cover and more terrain complexity than the Central and East ecoregions. We hypothesized that such characteristics affect remote sensing-based road detection capabilities, and thus, we used the ecoregions as strata for evaluating model performance under different conditions. We digitized the seven original regions from Philippon et al. (2019) along level 2 global administrative boundaries (FAO, 2015) and consolidated the four regions within DRC into a single region (East) because of the low rates of road development there.

2.2. Road definition

The majority of Congo Basin forest roads are associated with selective logging activities and located inside concession boundaries (Kleinschroth et al., 2019b; Kleinschroth and Healey, 2017). Here, road development typically involves the opening or reopening of wide primary and secondary haul roads, used by trucks to transport logs to mills or transport facilities, and narrower skid trails used by skidders and other logging equipment to bring felled trees to log landings located along haul roads (Kleinschroth and Healey, 2017). We focused our mapping effort on haul roads, which are the clearest visible feature of selective logging in satellite imagery.

Our road definition was based on visual interpretation of 4.8 m resolution quarterly and monthly Planet mosaics (Planet Team, 2017) and 10 m resolution Sentinel-2 imagery. For a forest disturbance to be defined as road development, we used the following requirements from Slagter et al. (2023) with minor adaptations:

- Clearing occurs in linear shapes, with appearance of bare soil.
- Clearing is composed of spatially continuous canopy openings with little interruption.
- Clearing needs to be visible in Planet mosaics (at 4.8 m resolution) as well as in Sentinel-2 imagery (at 10 m resolution).
- Clearing stays visible for at least 6 months before canopy recovers or vegetation reestablishes on bare soil.

The last criterion was included to effectively define haul roads inside logging concessions, separating them from skid trails, which were not included in our road definition. Skid trails can in some cases also cause narrow linear disturbances that appear similar to roads, which may cause confusion during visual interpretation. However, skid trails do not involve the opening of canopy and their visibility usually fades quickly, opposed to the longer-lasting visibility of haul roads. For this reason, a 6-month minimum visibility criterion was adopted as a functional definition to distinguish between haul roads and skid trails in satellite imagery. Roads developed for non-logging purposes (e.g., new transportation corridors or mining roads) were also within our road definition and not separately distinguished from logging roads.

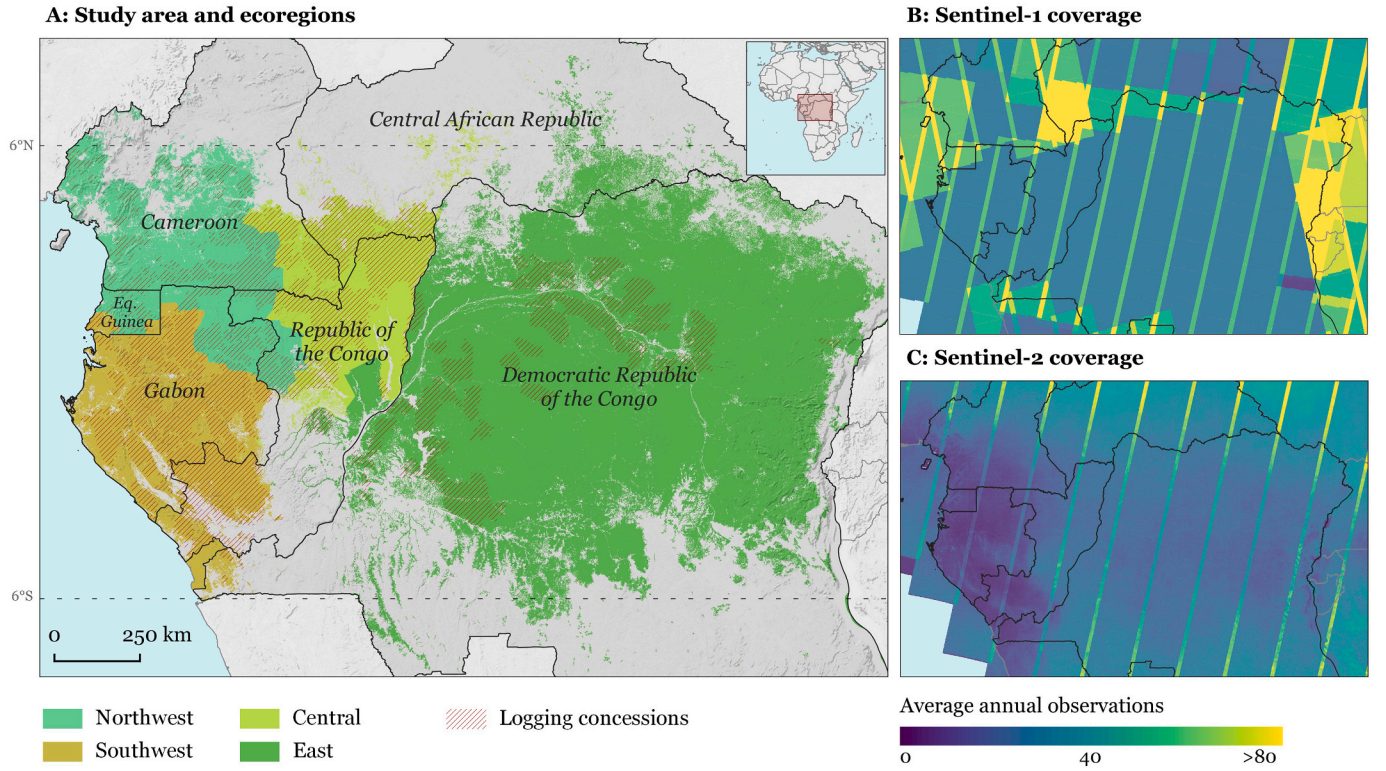

Fig. 3. Overview of the study area, the four defined ecoregions (adopted from Philippon et al., 2019) and the locations of logging concessions (A), the Sentinel-1 data coverage (B), and the cloud-free Sentinel-2 data coverage (C) for 2019-2022.

2.3. Input data and preprocessing

We sourced Sentinel-1 and -2 satellite imagery through Google's cloud-based geospatial processing platform Google Earth Engine (GEE) (Gorelick et al., 2017). The Sentinel-1 satellites consistently acquire C-band radar imagery independent from daylight and cloud cover conditions with 6-12 days revisit time (Torres et al., 2012). We used the Ground Range Detected (GRD) imagery acquired in Interferometric Wide Swath mode. The images have a spatial resolution of approximately 20 × 22 m and are provided with 10 m pixel spacing. Sentinel-1 images in GEE have been preprocessed by the application of the orbit files, thermal noise and GRD border noise removal, radiometric calibration to sigma naught and range-Doppler terrain correction, based on the European Space Agency's Sentinel-1 Toolbox methods (European Space Agency, 2022). We further preprocessed the images by removing remaining border noise at scene edges and by removing edge noise at the sensor's acquisition start and end in each orbit path.

The Sentinel-2 satellites acquire optical imagery with 5 days revisit time in the visible, near-infrared and short-wave infrared portions of the electromagnetic spectrum at 10-20 m spatial resolution (Drusch et al., 2012). We used the Level 1C Top of Atmosphere (TOA) and Level 2A Surface Reflectance (SR) imagery. We preprocessed the images by applying cloud- and shadow masking, following the GEE-based methods from s2cloudless (Zupanc, 2017), using a 40% cloud-probability threshold. Additionally, we detected cloud shadows based on low near-infrared reflectance in proximity of detected clouds and the solar azimuth angle. To remove errors in the cloud- and shadow masks, we applied a 5 × 5 pixel focal majority filter and expanded the resulting masks with a 50 m buffer.

For Sentinel-1, we selected both the VV and the VH polarizations scaled to dB. For Sentinel-2, we computed the Normalized Difference Vegetation Index (NDVI) and the Normalized Burn Ratio (NBR) based on red, near-infrared and short-wave infrared reflection. These indices were expected to strongly highlight the contrast between intact forests (characterized by dense canopy) and roads (characterized by bare soil visibility).

Additionally, we produced a 30 m resolution slope layer from the Shuttle Radar Topography Mission (SRTM) (Farr et al., 2007). We expected slope information to be of value for the model, because road opening practices are commonly restricted by terrain and slope conditions in mountainous areas.

2.4. Change ratios

We produced a 4-year time series of Sentinel-1 and -2 change ratios for January 2019 until December 2022, by comparing backscatter and spectral reflectance of 3-monthly averages (monitoring periods) with a 2-year historical median (baseline period). Change ratios have frequently and succesfully been applied to radar imagery for forest change detections (e.g., Bouvet et al., 2018; Carstairs et al., 2022; Dupuis et al., 2023; Tanase et al., 2018). In this study, we applied the same approach for optical imagery based on the NBR and NDVI. The resulting 3-monthly averaged change ratios based on VV, VH, NBR and NDVI strongly highlight forest changes such as newly opened roads. Furthermore, in contrast to analyzing individual images, the use of change ratios largely reduces the need for complex preprocessing steps to correct for factors like atmospheric conditions – affecting Sentinel-2 TOA imagery, and speckle and terrain – affecting Sentinel-1 imagery.

Road openings are highlighted in change ratios by a sharp decrease in NBR and NDVI in linear shapes (Fig. 4 B3 and C3). A decrease in VV and VH backscatter can also be observed at road locations due to a radar shadowing effect. This effect occurs at sharp edges between forest and non-forest, resulting in an area that cannot be reached by the radar pulse. A linear-shaped backscatter decrease can also be accompanied by a backscatter increase, due to increased double-bounce effects, direct scattering and layover. The effects of backscatter decrease and increase at road locations are caused by the side-looking nature of radar sensors, and the occurrence of this effect relates to the road orientation relative

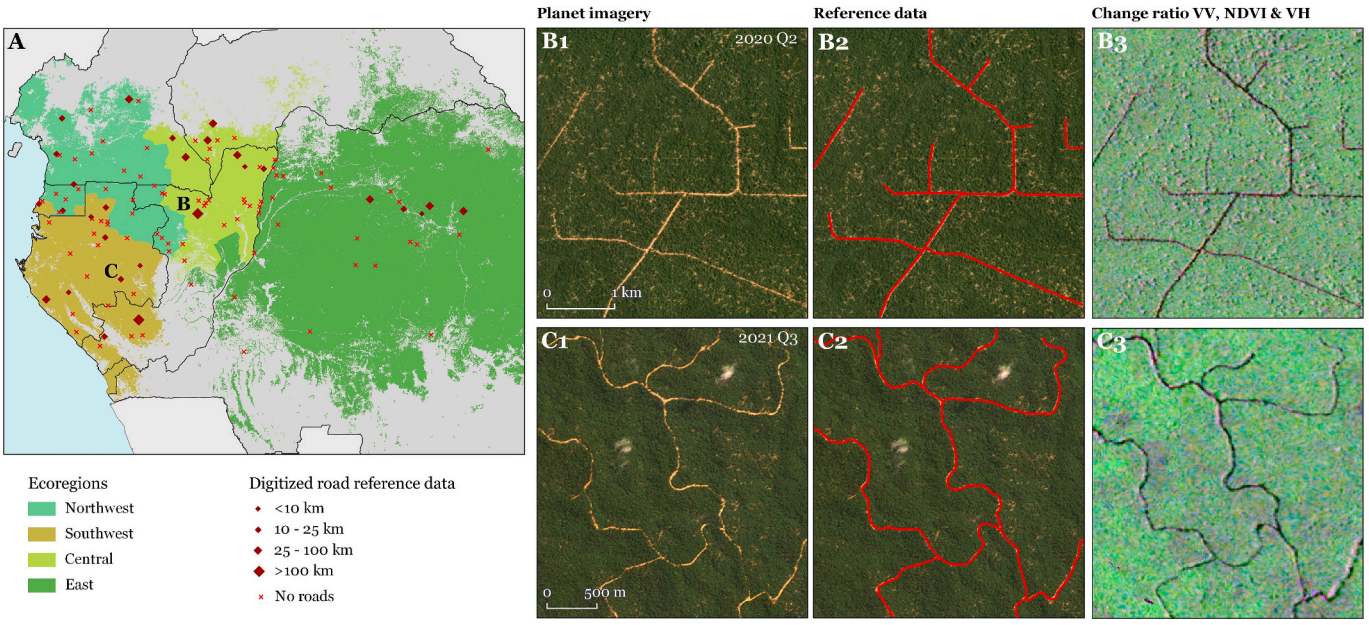

Fig. 4. Overview of the reference data locations in the four ecoregions (A), detailed examples of the manual digitization of reference data (B1, B2, C1 and C2), and RGB visualizations of the corresponding change ratios computed for a 3-month period immediately after completion of the specific road openings (B3 and C3).

to the sensor (Touzi and Sasitiwarih, 2001).

We produced the time series of 3-monthly averaged change ratios in time steps of one month, allowing temporal overlap in subsequent change ratios. In this way, we simulated a monitoring scenario that can be used in practice for monthly updated road maps. We developed the change ratios for the years 2019 and 2020 based on a 2-year historical median computed for 2017 and 2018, using Sentinel-1 and Sentinel-2 TOA imagery. We developed the change ratios for the next two years 2021 and 2022 based on a historical median from 2019 and 2020, using Sentinel-1 and Sentinel-2 SR imagery. This separation in baseline periods was made in order to leverage the higher-quality Sentinel-2 SR imagery for the latter two years, that is not available prior to 2019. For consistency, we made the same separation of baseline periods for Sentinel-1 change ratios.

2.5. Reference data

To train, validate and test our model, we produced an extensive reference dataset throughout the four defined ecoregions in the Congo Basin forest (Fig. 4). We identified areas with active road development in logging concessions (Global Forest Watch, 2024) and manually digitized roads opened in 2020, 2021 and 2022. We did not include existing roads from pre-2019 in our reference data, because we aimed to train our model for only detecting new road openings as highlighted in change ratios.

In addition to the training data from locations with road development, we specifically included regions with forest changes not related to road development, caused by, for example, agriculture, mining, windthrows or rivers, to ensure that the model could be sufficiently trained to distinguish road development from other forest changes. We expected such locations to be typical 'edge cases' that would be particularly challenging for the model to interpret, possibly leading to false road detections when not sufficiently represented in the training data. Within the extent of our collected reference data locations, we randomly sampled 6400 image chips of 128 × 128 pixels. This sample was evenly distributed for locations with and without roads present and also evenly distributed among the four ecoregions, to ensure a reliable comparison of model performance per ecoregion.

For each image chip, we produced change ratios based on Sentinel-1 and -2 imagery to be used as an input for model training, validation and testing. We included the Sentinel-1 change ratios based on VV and VH, the Sentinel-2 change ratios based on NDVI and NBR, derived both from SR and TOA images, and the slope computed from the SRTM. We rasterized the manually digitized roads with a width of 3 pixels (i.e., ~30 m) to be included as class labels of road and non-road pixels.

It was of high importance that the change ratios produced at each reference data location were based on a baseline period preceding the road opening and a monitoring period shortly after the completion of all road opening activities, to ensure that the change ratios matched with the actual moment of road opening. For this reason, we labelled each reference data location with a generic road opening start and end date, based on visual interpretation of Planet and Sentinel-2 imagery. Then, at each reference data location, we computed the corresponding change ratios for the three months immediately following the road opening end date, with a baseline period of the two years preceding the road opening start date. It was also important to ensure that the earliest opened roads at the reference data locations would still be clearly visible in the corresponding change ratios. Therefore, we only selected reference data locations where the time period between the road opening start and end date did not exceed one year (i.e., before vegetation regrowth obscured the earliest road openings). For the reference data locations without road presence, we selected random time periods to produce change ratios.

2.6. Model architecture and training

We built a CNN in Keras based on a U-Net model architecture (Ronneberger et al., 2015) to segment road pixels and non-road pixels in change ratios derived from Sentinel-1 and -2 imagery. The model consisted of three down- and upsampling blocks. Each downsampling block was composed of two convolution layers with batch normalization, max pooling and spatial dropout. Each upsampling block was composed of a transposed convolution layer, concatenation, spatial dropout, and two convolution layers with batch normalization.

Since the training data was highly imbalanced, containing a majority of non-road pixels, we trained the models using Dice Loss (Sudre et al., 2017). We selected a batch size of 32, Adam optimization (Kingma and Ba, 2015) with an initial learning rate of 0.001 and a learning rate decay of factor 4 after 6 epochs of no improvement, and applied early stopping after 15 epochs of no improvement.

We augmented our training dataset by mirroring each image chip horizontally, doubling our data volume. Mirroring the images also aided to artificially train the model to interpret 'side-looking' Sentinel-1 imagery acquired in either ascending or descending mode. In each batch during model training, we also randomly selected images to be adapted with random noise in the Sentinel-1 bands, to reduce risks of model overfitting on remaining speckle. We also randomly selected either the TOA or the SR bands from Sentinel-2 images in each batch to ensure that the model simultaneously learned road representations in both Sentinel-2 data types. All data augmentations and the random selection of TOA or SR were only done at the stage of model training.

To train and evaluate the model, we split our reference data in training, validation and testing portions. These partitions were made at the level of the reference data locations (Fig. 4), to ensure no spatial overlap between sampled image chips used for training, validation and testing. Validation data (15%) was used to optimize model parameters and applying learning rate decay, early stopping and restoring the model weights of the best-performing epoch. Testing data (10%) was held-out to evaluate different model configurations based on the use of Sentinel-1 bands only, Sentinel-2 bands only, and the combination of both sensors (as described in section 2.8). The final model applied at large scale was trained with 85% training data and 15% validation data and evaluated in and independent accuracy assessment (as described in section 2.9).

2.7. Model application to Congo Basin forest

We applied our model in GEE to monitor road development across the six Congo Basin countries from January 2019 until December 2022. Separate road detections were produced for each monthly change ratio time step.

Next, all monthly road detection images were overlaid and only pixels with at least three detections within a window of four months were retained, to create a road map representing only confident and repeated detections. We assigned the month of the change ratio that first detected the road as the road opening date for each detected pixel. Road detections for the first three months of 2023 were additionally processed to ensure that repeated detections of late-2022 road openings were retained. We also applied our model for 2018 (i.e., the year before our monitoring started) and removed all road pixels detected in that year in order to avoid a peak in detections in our first monitoring month in 2019 that would stem from road openings already established in 2018.

We removed road detections within 100 m of potential surface water, to exclude areas where variable water levels or active stream channel migration may create linear features that resemble roads. We mapped potential surface water as areas with water occurrence in at least 5% of months in the JRC Global Surface Water Mapping Layers v1.4 1984-2021 dataset (Pekel et al., 2016), occurring within the Global Channel Belt dataset (Nyberg et al., 2023), or typed as *permanent water, water gain, water loss, dry period, wet period, stable seasonal, high frequency,* or *probable permanent water* in the GLAD Global Surface Water Dynamics 1999-2021 dataset (Pickens et al., 2020b). Additionally, we removed all road detections at the edges of the forest baseline map. We also removed small isolated detections, with no other road detection clusters within 2.5 km distance.

To fill small gaps and missing connections in the road map, we applied a dilation and erosion step with a 5-pixel radius. We used neighborhood statistics to assign a detection date value to each pixel based on a 10-pixel majority. Finally, we vectorized the raster output, connected road segment endpoints within 200 m distance of each other and removed remaining unconnected segments shorter than 500 m.

2.8. Model performance evaluation

We evaluated the use of Sentinel-1 bands only, Sentinel-2 bands only, and the combination of both sensors per ecoregion, to gain a deeper understanding in the sensor's capacities for road detection. We trained separate models per sensor (-combination) in 10 folds, each with a different random split of training (75%), validation (15%) and testing data (10%) to obtain robust results for the comparisons. In each fold, based on the testing data, we computed precision (the proportion of detected road pixels that was correctly identified) and recall (the proportion of actual road pixels that was correctly detected), and averaged the results.

2.9. Accuracy assessment

We assessed the accuracy of the wall-to-wall Congo Basin forest road map based on a stratified random sample. This process was aimed at obtaining a statistical accuracy assessment of our map and was separate from the model testing described in section 2.8. Throughout the study area, we produced a grid of 1 × 1 km square blocks containing at least 50% forest cover in the forest baseline map. We divided the grid into two strata: one stratum containing blocks with road detections, and one stratum containing blocks without road detections. We randomly sampled 200 blocks in each stratum (Table 1). In each of the sampled 1 × 1 km blocks, we manually digitized all road openings within forests between 2019 and 2022, based on visual interpretation of Planet and Sentinel-2 imagery, following the same definitions as described in section 2.2.

We tailored our accuracy assessment for evaluating maps composed of line features. This is inherently different from common remote sensing-based outputs, which are usually maps composed of pixels. For that reason, conventional accuracy assessment methods (e.g., sampling random points, or presenting an Overall Accuracy) cannot be applied to our map. To assess the accuracy of our road map, we compared our mapped roads with the manually digitized roads in the sampled 1 × 1 km square blocks and calculated the true positives (TP), false positives (FP) and false negatives (FN) in units of road length. Then, we computed the rate of false detections (as a proportion of the total mapped roads), the rate of missed detections (as a proportion of the total manually digitized roads) and the F1 score.

$$F1\ score = \frac{2TP}{2TP + FP + FN}$$

We maintained a 50 m tolerance buffer for errors between our mapped roads and manually digitized roads. The accuracy metrics were calculated separately per ecoregion. Some of our road detections originated from road-related disturbances that were technically not within our definition of road opening, that could also not be clearly defined as false detections. To gain a deeper understanding of detections of all road-related phenomena occurring in our map, we digitized the following classes and reported their detection rates separately:

- Pre-existing road: Roads that were already established before 2019 (not considered as a false detection).
- Pre-existing road widening: Roads that were already established before 2019, which became widened, improved or paved during monitoring (not considered as a false detection).

Table 1
Distribution per stratum and ecoregion of the randomly sampled 1 × 1 km blocks for the accuracy assessment.

	Stratum 1 (road detections)	Stratum 2 (no road detections	Total
Congo Basin forest	200	200	400
- Northwest	60	24	84
- Southwest	82	30	112
- Central	40	15	55
- East	18	131	149

- Road opening followed by clearing: Roads that were only used as access roads for follow-up forest clearing, e.g., for mining or large-scale agriculture (not considered as a false detection).
- Road or skid trail not exceeding the 6-month visibility threshold: Small and quickly disappearing linear clearings with too short visibility duration to be within our road definition (considered as a false detection).

We also assessed the accuracy of our mapped total road length in the Congo Basin forest. For each sampled block, we compared the mapped road lengths with the manually digitized road lengths and computed the differences. Using this information, we estimated the level of overestimation or underestimation of road lengths in our map with a 95% confidence interval. For this comparison, the road types listed above were excluded from the manually digitized road lengths.

Additionally, we evaluated how an improved road detection timeliness affected the detection accuracies. We applied different thresholds for the per-pixel required number of road detections within different time window lengths and computed the resulting false detection rates, missed detection rates and F1 scores.

2.10. Spatial analyses

For the presented Congo Basin forest road map, we investigated the total road development lengths and densities per country. We also labelled different road characteristics and locations based on intersection with additional spatial datasets, including logging concessions (Global Forest Watch, 2024), protected areas (UNEP-WCMC and IUCN, 2022) and IFLs as defined for 2016 (Potapov et al., 2017). In addition, we assessed the overlap of our mapped roads with road inventories from pre-2019 to identify old road reopening, as opposed to roads that were newly opened. For this assessment, we used the manually digitized Congo Basin forest road map from Kleinschroth et al. (2019b) and forestry tracks mapped in OpenStreetMap until 2019 (OpenStreetMap contributors, 2024). Since these pre-2019 road maps have a coarser spatial detail, we buffered the road segments in the maps by 500 m before intersecting them with our map.

3. Results

3.1. Model performance evaluation

We observed a high variation for our road detection model performance based on the use of Sentinel-1 bands only, Sentinel-2 bands only, and the combination of both sensors (Table 2). In general, the combination of Sentinel-1 and -2 imagery yielded the best results in all ecoregions. The model performed better in the Central and East ecoregions in contrast to the Northwest and Southwest ecoregions.

Table 2
Performance of the road detection model applied to the held-out testing dataset. The precision and recall are reported for the entire testing dataset and for subsets of the testing dataset per ecoregion and were averaged for 10 folds. It should be noted that these numbers solely reflect on the model's pixel-level road segmentation capabilities for the reference data locations, which consisted of examples that were expected to be particularly challenging for the model. The numbers should only be interpreted for intercomparison and not as a measure for map accuracy, which is presented in Table 4.

	Sentinel-1		Sentinel-2		Sentinel-1 & -2	
	Precision	Recall	Precision	Recall	Precision	Recall
Congo Basin forest	0.667	0.666	0.749	0.659	0.750	0.751
- Northwest	0.579	0.548	0.717	0.577	0.715	0.622
- Southwest	0.701	0.654	0.730	0.371	0.732	0.721
- Central	0.698	0.746	0.748	0.870	0.762	0.853
- East	0.679	0.754	0.779	0.907	0.797	0.890

Within the Southwest ecoregion, which is characterized by high cloud cover and relatively complex terrain, the use of Sentinel-1 showed a large advantage over Sentinel-2 in terms of recall (i.e., fewer missed detections). In the Central and East ecoregions, which are characterized by flatter terrain and less cloud cover, the use of Sentinel-2 outperformed the use of Sentinel-1 by a large margin, mostly attributable to improvements in recall (i.e., fewer missed detections). For the Northwest ecoregion, the use of Sentinel-2 mainly led to an improved precision (i.e., fewer false detections) compared to the use of Sentinel-1.

We observed that terrain complexity and cloud cover were of major influence on model performance (Table 3). When the Sentinel-1 and -2-based model was applied to a subset of testing image chips with an average slope of at least 10°, the precision and recall dropped to 0.605 and 0.550 respectively (i.e., more false and missed detections). Such conditions were primarily observed in the Southwest and Northwest ecoregions, where respectively 51% and 14% of the data was in areas with steep slopes. For a subset of severely cloud-covered testing image chips, with at least 50% of its pixels cloud-masked, the precision and recall dropped to 0.703 and 0.648 respectively (i.e., more missed detections in particular). Such conditions occurred exclusively in the Southwest and Northwest ecoregions, where respectively 55% and 6.6% of the data was still severely cloud-covered in 3-month composites.

3.2. Accuracy assessment

A wall-to-wall Congo Basin forest road map was produced with a model based on the combination of Sentinel-1 and -2 imagery. The accuracy assessment of this map, based on randomly sampled 1 × 1 km blocks in a stratum containing road detections, revealed a false detection rate of 4.2%, a missed detection rate of 14.9%, and an F1 score of 0.909 (Table 4). The samples within the stratum containing no detected roads did not reveal any missed detections. Accuracies in the Central and East ecoregions were higher than in the Northwest and Southwest ecoregions. Considering the mapped length of all road types as listed in Table 5, our reported road length was likely underestimated by 3.5% (±9.2) for the stratum containing road detections.

Out of all mapped roads within our sampled blocks (157.0 km), 2.7% were fragments of pre-existing roads, 5.4% were related to pre-existing road widening, and 3.9% were related to the development of access roads that were quickly followed by a full forest clearing (Table 5), which were all not considered as false detections. Over a quarter of our false detections originated from roads or skid trails that should have been ignored by the model because they did not exceed the 6-month visibility threshold we set in our road definition.

All presented accuracies are based on the requirement that a road was detected at least three times within a time window of four months, to ensure a certain confidence in the final map. Increasing the road detection timeliness by requiring a lower number of subsequent detections led to increased false detections and decreased missed detections (Fig. 5). In contrast, more confident, but less timely, road detections could be achieved by requiring more subsequent detections. This leads to decreased false detections and increased missed detections.

Table 3
Performance of the Sentinel-1 and -2-based road detection model for areas with different slope and cloud cover conditions. The precision and recall are reported for specific subsets of the testing dataset with high cloud cover, low cloud cover, high average slope and low average slope and were averaged for 10 folds.

	Precision	Recall
All areas	0.751	0.750
High slope (>10°)	0.605	0.550
Low slope (<5°)	0.786	0.882
High cloud cover (>50%)	0.703	0.648
Low cloud cover (<5%)	0.784	0.835

Table 4
Overview of the accuracy assessment of the Congo Basin forest road map. The accuracies are based on the stratum containing road detections.

	False detection rate (%)	Missed detection rate (%)	F1 score
Congo Basin forest	**4.2**	**14.9**	**0.909**
- Northwest	6.9	18.0	0.889
- Southwest	4.0	19.2	0.884
- Central	1.7	5.0	0.966
- East	0.3	10.8	0.944

3.3. Congo Basin forest road map

The presented Congo Basin forest road map contains 35,944 km of road development between 2019 and 2022. (Fig. 6, Table 6). We estimate the actual road development length to be 37,201 km (±3310), based on the level of road length underestimation in our map. The vast majority of roads (27,858 km, 78%) were mapped inside logging concessions and located in the western part of the Congo Basin forest. Gabon (12,595 km), Cameroon (9844 km) and RoC (8358 km) had the highest numbers of road development. We observed that the annual length of road development in the Congo Basin forest was 7846 km in 2019, increasing gradually to 10,196 km in 2022 (Fig. 7).

The annual road development density throughout the Congo Basin forest was 4.9 m/km^2 forest between 2019 and 2022 (Table 6). The density was particularly high in Equatorial Guinea (17.6 m/km^2 forest), Gabon (13.6 m/km^2 forest) and Cameroon (12.7 m/km^2 forest), while DRC had a relatively low density (0.5 m/km^2 forest).

Based on an overlay with pre-2019 road maps, we estimate that approximately 10,800 km (30%) of our mapped roads can be related to reopening of old logging roads (Table 6). Road reopening occurred mostly in Gabon (40%). A large share of road development (8143 km) occurred within areas defined as IFL in 2016. The highest numbers of IFL encroachment due to road development were observed in RoC (3118 km) and Gabon (2211 km). In DRC, a country containing large areas of IFLs, approximately half of the road development (52%) was located within an IFL. Relative to the countries' remaining IFL size, the highest encroachment rates were observed in Equatorial Guinea (41.2 m/km^2 IFL) and Cameroon (38.3 m/km^2 IFL). We detected limited road development (878 km) in protected areas, of which most (590 km) was located in protected areas overlapping with logging concessions.

4. Discussion

4.1. Monitoring road development with Sentinel-1 and -2

Continuous and automated road mapping is one of the most urgent conservation needs for tropical forests today (Engert et al., 2024). Our study provides a novel method for large-scale monitoring of road development, based on a deep learning model trained with change ratios derived from Sentinel-1 and -2 imagery. This presents a substantial advancement compared to previous road mapping efforts based on manual digitization (e.g., Brandão and Souza, 2006; Engert et al., 2024; Gaveau et al., 2014, 2021; Kleinschroth et al., 2019b; Laporte et al., 2007) and generic remote sensing-based forest disturbance alerting systems (e.g., Doblas et al., 2022; Mermoz et al., 2021; Pickens et al., 2020a; Reiche et al., 2021).

The high spatiotemporal resolution of Sentinel-1 and -2 imagery enabled us to produce a highly detailed map of Congo Basin forest road development (Fig. 6), including narrow and transient logging roads. This introduces an unprecedented view on recent road developments, which are likely to have been largely left undetected by current state-of-the-art pantropical systems that track forest changes (e.g., Hansen et al., 2013, 2016; Reiche et al., 2021; Vancutsem et al., 2021) (Fig. 8). Our total length of mapped road development is also remarkably high in comparison to earlier mapping efforts in the Congo Basin forest. For example, we mapped 35,944 km of road development covering only four years (2019-2022), while Kleinschroth et al. (2019b) mapped 87,533 km covering 14 years (2003-2016) based on manual digitization. While some of the difference may be driven by increasing road development over time, the higher road numbers presented in our map likely stem from an improved level of detail, leading to a more complete map. This underscores the value of our automated detection methods for more detailed road monitoring in the future.

Our study highlights the complementary qualities of Sentinel-1 and -2 imagery, which combined led to the best road detection results (Table 2). This confirms the value of multi-sensor approaches for tropical forest applications (Joshi et al., 2016; Reiche et al., 2016). However, in regions with relatively little cloud cover and little terrain complexity (such as the Central and East ecoregions), Sentinel-2 imagery proved to

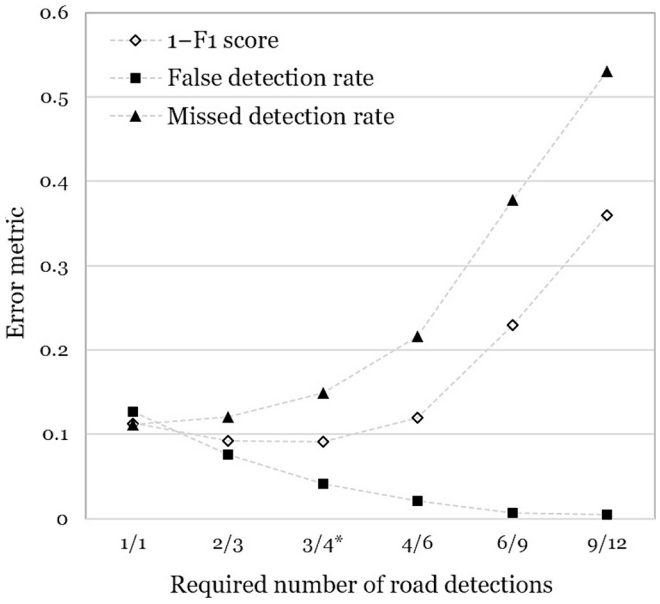

Fig. 5. Different scenarios for the required number of repeated monthly road detections and their resulting accuracies. Improving detection timeliness by decreasing the required number of detections leads to more false and less missed detections. * = the map presented in this study, resulting in the best F1 score.

Table 5
Overview of the different road types presented in our accuracy assessment, including a detailed breakdown of the true and false road detections.

		Northwest	Southwest	Central	East	Total
Total mapped roads within sampled blocks (km)		52.54	56.04	32.49	15.95	**157.02**
True detections (km, %)	Meeting our definition of road opening	37.64 (71.6%)	47.86 (85.4%)	31.13 (95.8%)	15.07 (94.5%)	**131.70 (83.9%)**
	Pre-existing road	4.14 (7.9%)	0.03 (0.1%)	0.00 (0.0%)	0.00 (0.0%)	**4.17 (2.7%)**
	Pre-existing road widening	1.81 (3.4%)	5.85 (10.4%)	0.80 (2.5%)	0.00 (0.0%)	**8.46 (5.4%)**
	Road opening followed by clearing	5.27 (10.0%)	0.06 (0.1%)	0.00 (0.0%)	0.84 (5.3%)	**6.17 (3.9%)**
False detections (km, %)	Road or skid trail not exceeding 6-month visibility threshold	0.76 (1.4%)	0.55 (1.0%)	0.56 (1.7%)	0.00 (0.0%)	**1.87 (1.2%)**
	Other	2.91 (5.5%)	1.69 (3.0%)	0.01 (0.0%)	0.04 (0.3%)	**4.65 (3.0%)**

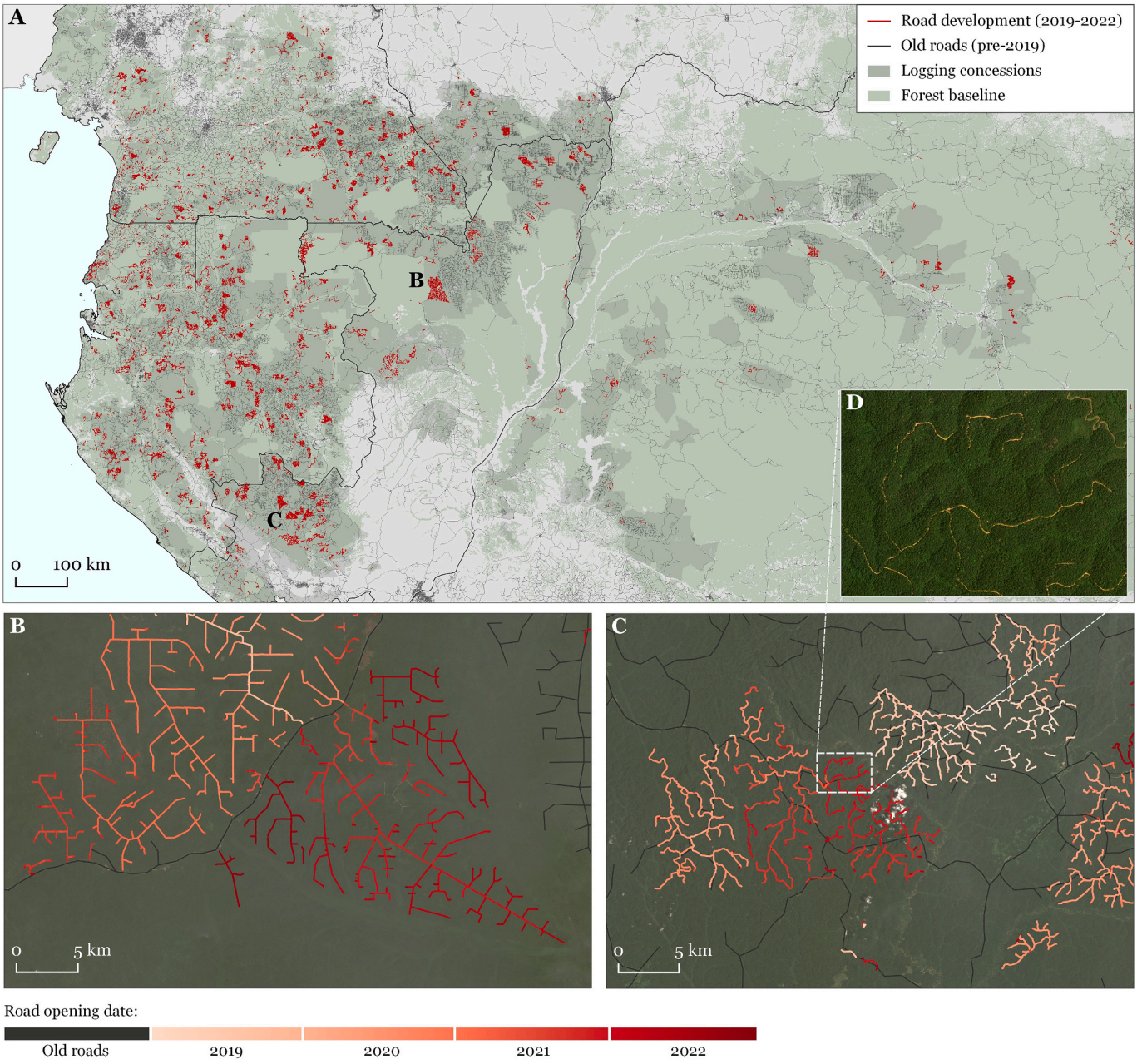

Fig. 6. Road development mapped between 2019 and 2022 in the Congo Basin forest (A), with spatiotemporally detailed examples of road development in two different ecoregions (B, C, D). Old roads were sourced from Kleinschroth et al. (2019b). Planet imagery is shown as a background. A detailed overview of this map can be viewed at: https://nrtwur.users.earthengine.app/view/forest-roads.

Table 6
Overview of road lengths mapped in the Congo Basin forest. Road characteristics and locations are provided per country.

	Total road length (km)	Annual road development density (m/km^2 forest)	Road reopening estimate (km, %)	Located inside logging concessions (km, %)	Located in intact forest landscapes (km, %)	Located in protected areas (km, %)
Congo Basin forest	35,944	4.9	10,800 (30.0%)	27,858 (77.5%)	8143 (22.7%)	878 (2.4%)
Cameroon	9844	12.7	2722 (27.7%)	6412 (65.1%)	1361 (13.8%)	91 (0.9%)
Central African Republic	1022	3.3	275 (26.9%)	1011 (98.9%)	125 (12.2%)	119 (11.6%)
RoC	8359	9.6	1864 (22.3%)	7663 (91.7%)	3118 (37.3%)	32 (0.3%)
DRC	2395	0.5	430 (18.0%)	1685 (70.3%)	1238 (51.7%)	146 (6.1%)
Equatorial Guinea	1723	17.6	466 (27.0%)	746 (43.3%)	88 (5.1%)	43 (2.5%)
Gabon	12,595	13.6	5040 (40.0%)	10,339 (82.1%)	2211 (17.6%)	447 (3.5%)

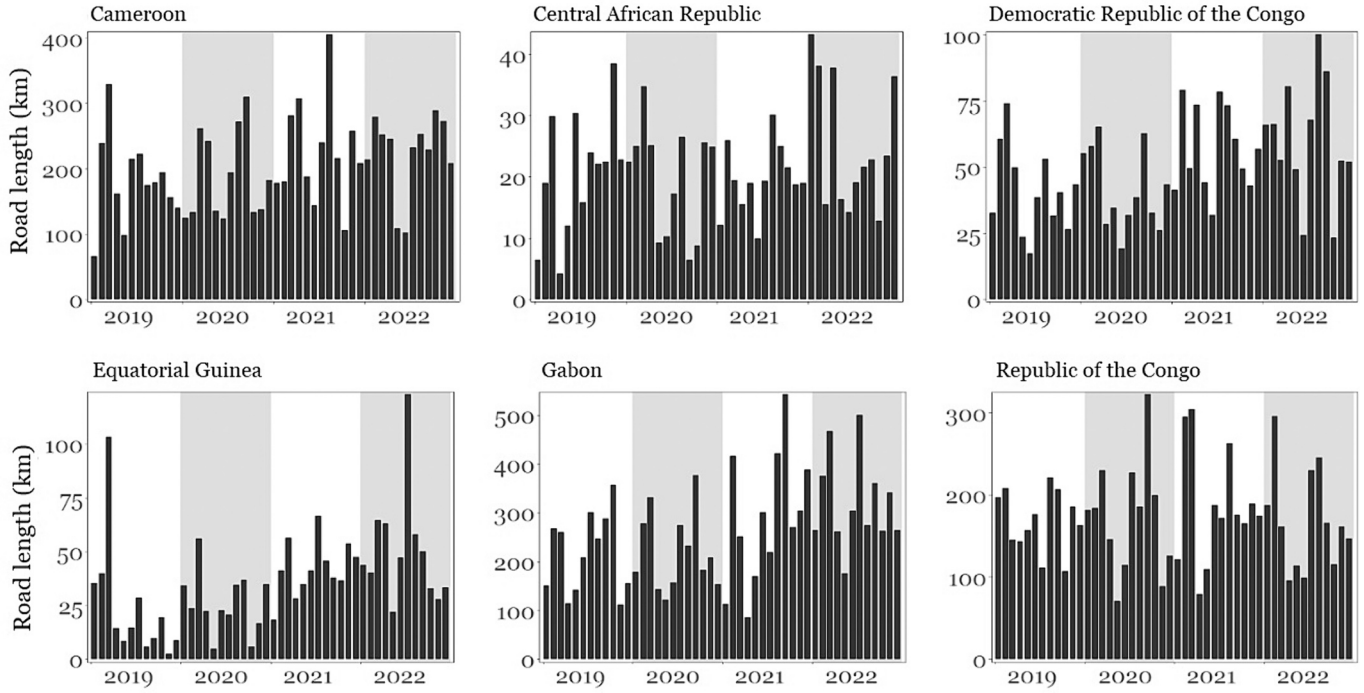

Fig. 7. Road development per month for the different countries in the Congo Basin forest for 2019-2022. Y-axes differ in scales.

be already highly accurate on its own, and the addition of Sentinel-1 imagery showed little added benefit. In general, the sensor-specific testing accuracies of our models revealed that Sentinel-2 imagery was indeed the most important data source for accurate road detections. Only in the heavily cloud-covered Southwest ecoregion, Sentinel-1 obtained higher accuracies compared to Sentinel-2, for which the 3-month composites were commonly severely obstructed by clouds. We hypothesize that, when weather conditions allow, nadir-oriented optical imagery is best at highlighting narrow road-related forest disturbances. In contrast, detecting roads with side-looking radar imagery is in many cases dependent on the occurrence of the linear shadowing and double-bounce effects at road edges, which are related to the incidence angle and in particular the road orientation (Touzi and Sasitiwarih, 2001). These effects do not occur for roads oriented 'towards' the radar sensor, and these may be missed.

The presented Congo Basin forest road map still showed some false road detections (4.2%) and missed road detections (14.9%). We hypothesize that these errors mainly stemmed from areas with frequent cloud cover or complex terrain. Cloud cover can cause long data gaps in the Sentinel-2 time series, which can result in delayed or missed road detections. Complex terrain requires complex road network layouts which are more challenging to detect accurately, while the terrain complexity itself also poses difficulties for remote sensing applications in general. We also observed some false detections caused by narrow meandering rivers, that were not captured by our surface water masking approach. The drawbacks of cloud cover and complex terrain became evident in the Southwest (F1 score: 0.884) and Northwest (F1 score: 0.889) ecoregions, leading to more missed detections. In contrast, much higher accuracies were observed for the Central (F1 score: 0.966) and East (F1 score: 0.944) ecoregions, dominated by flat areas, straight roads and little cloud cover. Although the missed detection rate of 14.9% is notable, we observed that most of these unmapped roads were only small segments (average length: 260 m) of correctly detected road networks.

Our study shows that change ratios derived from Sentinel-1 backscatter (VV and VH) and two Sentinel-2 indices (NDVI and NBR) are a solid basis for accurate detections of road development. Still, research aimed at the fundamental qualities of high-resolution radar and optical satellite sensors to detect small-scale disturbances like roads is ongoing (Dupuis et al., 2023; Hethcoat et al., 2021; Hoekman et al., 2020; Lima et al., 2019). The value of different Sentinel-1 and -2-based metrics could be studied, in particular in relation to various regional conditions like terrain, cloud cover or forest type, which affect road detection capacities.

For road monitoring in practice, the trade-off in detection timeliness versus accuracy should be considered (Fig. 5). For the maps presented in this study, roads are detected with high accuracies after a time lag of several months, which is considerably slower than than the detection timeliness of generic near real-time forest disturbance alerting systems (Doblas Prieto et al., 2023; Reiche et al., 2024). Still, more timely road detections can be obtained, which may be valuable for applications that require early warnings of forest changes, such as law enforcement (Finer et al., 2018; Lynch et al., 2013; Weisse et al., 2019). An increased detection timeliness, however, will lead to increased false road detections. For effective near real-time road detections, further research could address accurate road segmentation techniques based on single images.

We believe that the performance of our road detection model, in particular a reduction of the missed road detections, could be improved by the inclusion of more training data (though the digitization of training data is labor-intensive), developing region-specific models suiting different regional conditions, or specific model architectures tailored for segmenting connected road networks (e.g., Batra et al., 2019). Such improvements may also reduce the need for postprocessing steps as presented in this study, such as the removal of specific areas prone to false detections (e.g., surface water edges, forest edges), forcing connections between road gaps, or combining multiple road detection timesteps to increase detection confidence. It should be noted, however, that very narrow or subcanopy tracks will probably never be detectable with a basis of 10-20 m resolution satellite imagery, regardless of the model that is applied. Therefore, future efforts may adopt higher-resolution satellite data such as Planet imagery (e.g., Dalagnol et al., 2023) to enable more detailed detections of narrow roads and tracks.

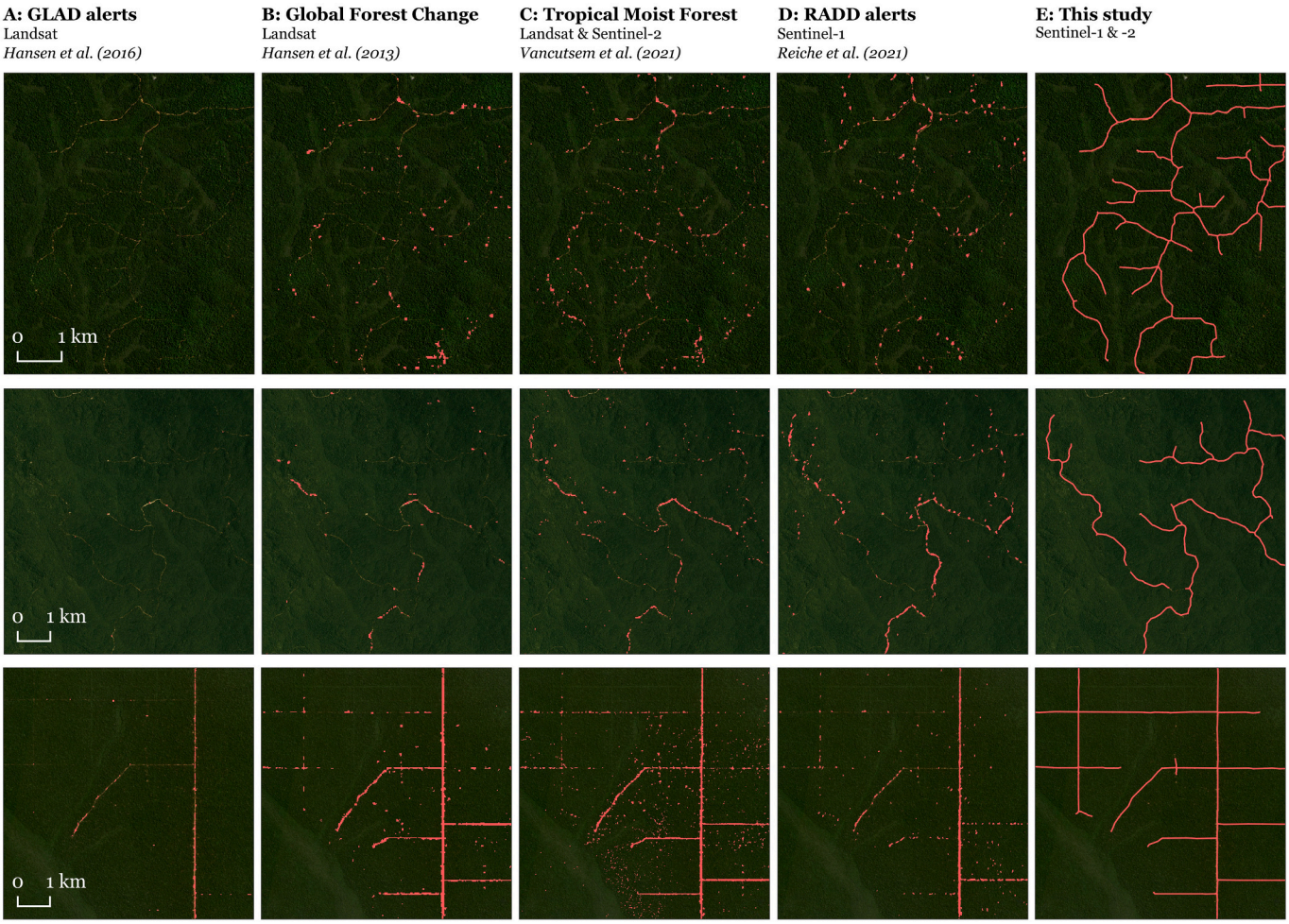

Fig. 8. Visual comparison of existing operational forest change products and our methods for the years 2019-2022. From left to right: GLAD high confidence alerts (A, Hansen et al., 2016), annual tree cover loss from the Global Forest Change product (B, Hansen et al., 2013), annual changes and transitions (deforestation and degradation) from the Tropical Moist Forest product (C, Vancutsem et al., 2021), RADD high confidence alerts (D, Reiche et al., 2021), and the road detection methods presented in this study (E). From top to bottom, these regions are located in Cameroon (central coordinate: 2.36°N, 12.89°E), Gabon (central coordinate: 0.28°S, 13.61°E), and RoC (central coordinate: 3.28°N, 17.51°E). Planet imagery is shown as a background.

4.2. Congo Basin forest road development

We mapped 35,944 km of road development in the Congo Basin forest between 2019 and 2022 with large regional differences (Fig. 6, Table 6). The majority of roads were located in the western countries Cameroon, Equatorial Guinea and Gabon, where logging concessions are widespread. The western regions also generally showed denser and more complex road development patterns than the central and eastern regions (Fig. 6 B and C), which may be linked to differences in terrain complexity and historic forest use patterns. We also observed temporal dynamics of road development throughout the years (Fig. 7), which may be linked to seasonal effects, because road opening primarily happens in the dry season (Gou et al., 2022; Vargas et al., 2019).

The logging activities in the Congo Basin forest were the major driver of road development, with the majority of mapped roads (78%) located inside the boundaries of logging concessions (Table 6). This is in line with historical patterns in the region (Kleinschroth et al., 2019b), and it is likely that these transient roads will become abandoned after several years. As the most recently awarded concessions may not yet be present in the Global Forest Watch dataset we used, the real percentage of logging roads may in fact be even higher than 78%.

Notably, a substantial portion of road development (30%) may correspond to the reopening of old logging roads. We based this percentage on a comparison between our map and pre-2019 road inventories (Table 6, Fig. 9). Ecological impacts and carbon emissions of logging activities are much lower when old infrastructure is reused, compared to when entirely new roads are opened (Kleinschroth et al., 2016). Therefore, it is important to differentiate between new and reopened logging roads to understand impacts on the forest landscape and carbon emission patterns. Caution is required in drawing definitive conclusions about which roads are new or reopened based solely on the comparison of these two road maps. The pre-2019 road reference, which relied largely on manual digitization based on 30 m resolution Landsat imagery, is susceptible to spatial inaccuracies and may miss narrow or transient road segments, meaning that the road reopening practices may in fact be higher than the estimated 30%.

A large share of road development (23%) was located in areas defined as IFLs in 2016 (Potapov et al., 2017) (Table 6). Naturally, the highest percentages of road development in IFLs were observed for countries with relatively large remaining IFL extents, such as DRC, in contrast to countries where many forests have historically already been affected by human activity. Extensive road development in IFLs is somewhat expected, since they consist of many previously unlogged areas where the largest and 'best' trees are still available, making selective logging here economically attractive (Kleinschroth et al., 2019c). Only a small portion of road development in the Congo Basin forest (2.4%) was located in protected areas. Most of these roads were still located inside logging concessions overlapping with protected areas.

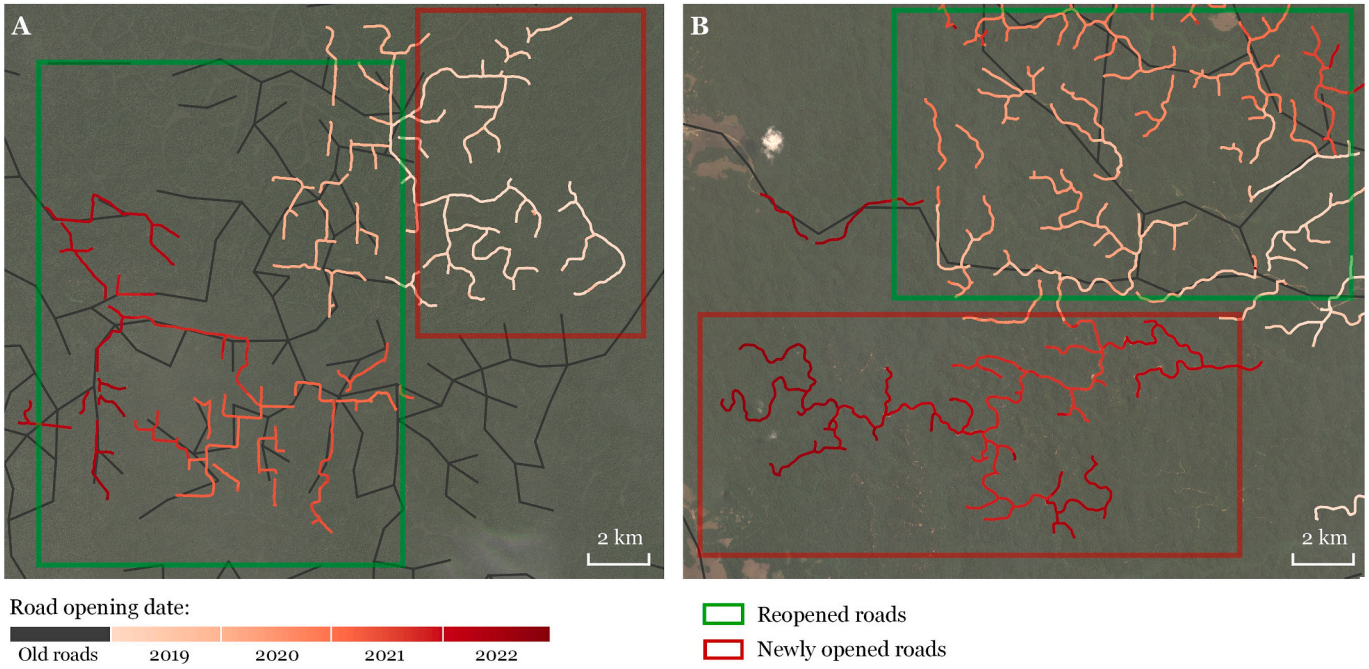

Fig. 9. Our road map overlaid with manually digitized roads from the 1970s until 2019 (Kleinschroth et al., 2019b), indicating where our road detections likely correspond to the reopening of old roads and where entirely new roads have been opened. A logging activity in Cameroon shows road reopening in the western part and newly opened roads in the northeastern part (A, central coordinate: 3.67°N, 14.64°E). A logging activity in Gabon shows partly road reopening in the northern part and newly opened roads in the southern part (B, central coordinate: 1.30°S, 13.60°E). Planet imagery is shown as a background.

Road development inside protected areas can also serve as infrastructure development in national parks (e.g., a detected road in the Odzala-Kokoua National Park in RoC seems to be developed to reach an eco-lodge).

Overall, we observed a slight increase in road development from 2019 to 2022 throughout the Congo Basin forest, particularly in Equatorial Guinea, Gabon and DRC. This may indicate that logging activities continue to expand, as has been the trend over the last decades (Kleinschroth et al., 2019b). However, for 2015-2020, Shapiro et al. (2023) estimated relatively stable levels of industrial logging in the Congo Basin forest. For more reliable estimates about trends in road development and logging activities, a consistent road mapping methodology conducted over a longer timeframe is needed.

4.3. Implications for forest monitoring applications

Detailed and regularly updated road maps generated through our automated monitoring methods can offer valuable insights into the spatial and temporal patterns of road development and evaluate their impact at large scale. First, detailed logging road maps could be used to spatially explicit assess ecological impacts and carbon emissions associated with selective logging activities (Gideon Neba et al., 2014; Pearson et al., 2014; Umunay et al., 2019). Road maps can also aid in formulating targeted strategies to mitigate climate impacts, such as improved road planning (Ellis et al., 2019; Putz and Pinard, 1993), which is a carbon emission reduction opportunity particularly for logging practices in the Congo Basin forest (Ellis et al., 2019; Umunay et al., 2019).

Furthermore, timely road monitoring can aid in preventing illegal forest activities. Government officials could use frequently updated maps to ensure that logging operations are in accordance with pre-harvest planning, complying with agreed concession borders and annual allowable cuts (Fig. 10). Practices of logging crews can be monitored and illegal road openings and logging activities may be stopped at an early stage. Forest managers could also use up-to-date road maps for targeted preventions of unauthorized post-logging activities in

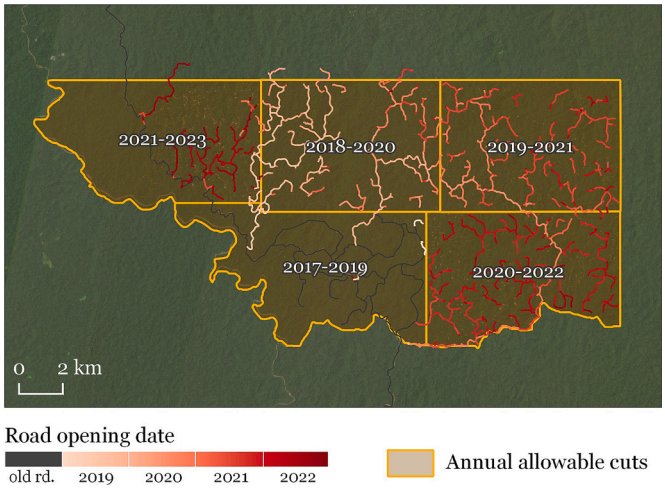

Fig. 10. A demonstration of how combining road monitoring methods with delineations of annual allowable cuts (assiéttes annuelles de coupe, AAC) in Gabon can aid in verifying whether logging operations are complying with pre-harvest planning and concession borders (central coordinate: 0.65°S, 11.93°E). Planet imagery is shown as a background.

opened-up forests like agricultural colonization, mining, poaching or artisanal logging (Kleinschroth and Healey, 2017; Laurance et al., 2009). For example, recently opened road networks could be mapped and access locations could be identified for road closures (Bicknell et al., 2015).

Finally, at larger scale, wall-to-wall road maps can improve delineations of terrestrial human footprints or forest intactness (Potapov et al., 2008, 2017; Riggio et al., 2020; Venter et al., 2016), which heavily rely on road maps as indicators. Currently, these metrics are typically based on visual interpretations of satellite imagery or existing road datasets and are therefore seriously incomplete or outdated (Barber

et al., 2014; Engert et al., 2024; Sloan et al., 2018), commonly overlooking narrow and transient roads. Despite their drawbacks, these human influence maps are widely adopted as measures for ecological integrity and habitat fragmentation. For example, IFL maps are integrated in the Forest Stewardship Council standard, with strong implications for forestry practices on the ground (Kleinschroth et al., 2019a; Zwerts et al., 2024). Our road monitoring methods can aid in creating automated, consistent, and more detailed maps delineating the extent of human influence almost in real time.

The presented methods for monitoring road development can potentially complement current operational forest disturbance alerting systems (e.g., Diniz et al., 2015; Doblas et al., 2022; Hansen et al., 2016; Mermoz et al., 2021; Pickens et al., 2020a; Reiche et al., 2021; Vargas et al., 2019; Watanabe et al., 2021). Small-scale disturbances like roads have historically been challenging to map and benefit from a separate method specifically aimed at road detections (Fig. 8). Furthermore, the thematic distinction of roads is a crucial aspect in further forest disturbance characterization, for example for disaggregating human-induced from natural disturbances or the characterization of logging activities (Dupuis et al., 2023; Welsink et al., 2023). Also, locations of new roads can be an important predictor for future deforestation and forest degradation and this information can aid in preventing illegal activity (WWF, 2022). The value of road monitoring is most apparent when detailed and regularly updated road maps are combined with additional datasets (Fig. 10, Table 6).

Beyond detecting only road (re)opening, it is crucial to enable similar methods to monitor road persistence. In practice, after a timber harvest, a large portion of logging roads is abandoned and revegetates naturally (Kleinschroth et al., 2015). For such roads, the negative secondary effects may be relatively minor, when proper post-harvest management, such as effective road decommissioning, is applied (Bicknell et al., 2015; Kleinschroth and Healey, 2017). Roads that remain open may have far more negative secondary effects. Therefore, continuous long-term monitoring of road development dynamics and comprehensive evaluation of road impacts should involve mapping both road (re)opening and their persistence. To monitor road abandonment, optical imagery can offer important information, since abandoned roads often rapidly revegetate and can be distinguished in remote sensing data based on their high photosynthetic activity, highlighted by a peak in near-infrared reflectance (Kleinschroth et al., 2015).

The adaptiveness of our road detection methods based on the combination of Sentinel-1 and -2 imagery to varying conditions indicates that our approach can be generally expanded to create road maps for all tropical regions. Still, the model presented is this study was trained specifically for the Congo Basin forest. For a transferable pantropical road detection model, additional training data from other continents, where road development patterns may be different, would likely be needed.

5. Conclusion

The ecological and climate impacts of roads in forests can be severe, and inventories of road development in remote tropical regions have been largely incomplete or outdated. This study introduced novel, automated methods to monitor road development in tropical forests on a monthly basis, leveraging the complementary value of high spatiotemporal resolution radar and optical satellite imagery. We successfully trained and applied a deep learning model to map road development for the Congo Basin forest with an unprecedented level of detail.

Our methods enable road mapping in an efficient, detailed, and timely updated way. This may serve several crucial forest management and conservation purposes. Operational road development monitoring can provide a basis for assessments of ecological impacts and carbon emissions related to logging, aid in preventing illegal forest activities, and provide a basis for improved understanding and evaluation of human impacts on tropical forests around the world.

CRediT authorship contribution statement

Bart Slagter: Writing – original draft, Visualization, Validation, Software, Methodology, Investigation, Funding acquisition, Formal analysis, Conceptualization. **Kurt Fesenmyer:** Writing – original draft, Visualization, Validation, Software, Methodology, Investigation, Funding acquisition, Formal analysis, Conceptualization. **Matthew Hethcoat:** Writing – review & editing, Visualization, Methodology, Formal analysis, Conceptualization. **Ethan Belair:** Writing – review & editing, Supervision, Funding acquisition, Conceptualization. **Peter Ellis:** Writing – review & editing, Supervision, Funding acquisition, Conceptualization. **Fritz Kleinschroth:** Writing – review & editing, Conceptualization. **Marielos Peña-Claros:** Writing – review & editing, Supervision, Funding acquisition, Conceptualization. **Martin Herold:** Writing – review & editing, Supervision, Funding acquisition, Conceptualization. **Johannes Reiche:** Writing – review & editing, Supervision, Methodology, Funding acquisition, Conceptualization.

Declaration of competing interest

The authors declare that they have no known competing financial interests or personal relationships that could have appeared to influence the work reported in this paper.

Data availability

The Congo Basin forest roads dataset (including its regular updates) is openly available via Zenodo: https://doi.org/10.5281/zenodo.13269839. More information about the forest road mapping project can be found at https://wur.eu/forest-roads.

Acknowledgements

This research was funded by Wageningen University's graduate school PE&RC and the Bezos Earth Fund. Additional funding was provided through the European Commission Horizon Europe project "Open-Earth- Monitor" (Grant number 101059548), Norway's Climate and Forest Initiative (NICFI), and the Open Domain Science project Forest Carbon Crime (Project Number: OCENW.M.21.203) of the Nederlandse Organisatie voor Wetenschappelijk Onderzoek (NWO). This work contains modified Copernicus Sentinel-1 & -2 data (2018–2023). Planet imagery was provided through the NICFI program and the Planet Education & Research program. We thank the Google Earth Engine team for providing sufficient cloud-computing capacities to complete this research. We thank Sytze de Bruin, Nandin-Erdene Tsendbazar, Laura Cué La Rosa (Wageningen University), Andreas Vollrath, Daniel Wiell (Food & Agriculture Organization) and Diego Marcos (Inria) for their assistance in completing this research. We thank the four anonymous reviewers for their comments to improve the manuscript.

References

Abdollahi, A., Pradhan, B., Shukla, N., Chakraborty, S., Alamri, A., 2020. Deep learning approaches applied to remote sensing datasets for road extraction: a state-of-the-art review. Remote Sens. https://doi.org/10.3390/RS12091444.

African Natural Resources Centre, 2021. Economic Performance of the Congo Basin's Forestry Sector.

Asner, G.P., Broadbent, E.N., Oliveira, P.J.C., Keller, M., Knapp, D.E., Silva, J.M.M., 2006. Condition and fate of logged forests in the Brazilian Amazon. Proc. Natl. Acad. Sci. USA 103, 12947–12950. https://doi.org/10.1073/pnas.0604093103.

Barber, C.P., Cochrane, M.A., Souza, C.M., Laurance, W.F., 2014. Roads, deforestation, and the mitigating effect of protected areas in the Amazon. Biol. Conserv. 177 https://doi.org/10.1016/j.biocon.2014.07.004.

Batra, A., Singh, S., Pang, G., Basu, S., Jawahar, C.V., Paluri, M., 2019. Improved road connectivity by joint learning of orientation and segmentation. In: Proceedings of the IEEE Computer Society Conference on Computer Vision and Pattern Recognition 2019-June, pp. 10377–10385. https://doi.org/10.1109/CVPR.2019.01063.

Bicknell, J.E., Gaveau, D.L.A., Davies, Z.G., Struebig, M.J., 2015. Saving logged tropical forests: closing roads will bring immediate benefits: peer-reviewed letter. Front. Ecol. Environ. https://doi.org/10.1890/15.WB.001.

Botelho, J., Costa, S.C.P., Ribeiro, J.G., Souza, C.M., 2022. Mapping roads in the Brazilian Amazon with artificial intelligence and Sentinel-2. Remote Sens. 14 https://doi.org/10.3390/rs14153625.

Bouvet, A., Mermoz, S., Ballère, M., Koleck, T., Le Toan, T., 2018. Use of the SAR shadowing effect for deforestation detection with Sentinel-1 time series. Remote Sens. 10, 1–19. https://doi.org/10.3390/rs10081250.

Brandão, A.O., Souza, C.M., 2006. Mapping unofficial roads with Landsat images: a new tool to improve the monitoring of the Brazilian Amazon rainforest. Int. J. Remote Sens. 27 https://doi.org/10.1080/01431160500353841.

Carstairs, H., Mitchard, E.T.A., McNicol, I., Aquino, C., Chezeaux, E., Ebanega, M.O., Dikongo, A.M., Disney, M., 2022. Sentinel-1 shadows used to quantify canopy loss from selective logging in Gabon. Remote Sens. 14 https://doi.org/10.3390/rs14174233.

Chen, Z., Deng, L., Luo, Y., Li, Dilong, Marcato Junior, J., Nunes Gonçalves, W., Awal Md Nurunnabi, A., Li, J., Wang, C., Li, Deren, 2022. Road extraction in remote sensing data: a survey. Int. J. Appl. Earth Obs. Geoinf. https://doi.org/10.1016/j.jag.2022.102833.

Dalagnol, R., Wagner, F.H., Galvão, L.S., Braga, D., Osborn, F., Sagang, L.B., da Conceição Bispo, P., Payne, M., Silva Junior, C., Favrichon, S., Silgueiro, V., Anderson, L.O., de Aragão, L.E.O.E.C., Fensholt, R., Brandt, M., Ciais, P., Saatchi, S., 2023. Mapping tropical forest degradation with deep learning and planet NICFI data. Remote Sens. Environ. 298, 113798 https://doi.org/10.1016/j.rse.2023.113798.

Diniz, C.G., Souza, A.A.D.A., Santos, D.C., Dias, M.C., Da Luz, N.C., De Moraes, D.R.V., Maia, J.S.A., Gomes, A.R., Narvaes, I.D.S., Valeriano, D.M., Maurano, L.E.P., Adami, M., 2015. DETER-B: the new Amazon near real-time deforestation detection system. IEEE J. Sel. Top. Appl. Earth Obs. Remote Sens. https://doi.org/10.1109/JSTARS.2015.2437075.

Doblas Prieto, J., Lima, L., Mermoz, S., Bouvet, A., Reiche, J., Watanabe, M., Sant Anna, S., Shimabukuro, Y., 2023. Inter-comparison of optical and SAR-based forest disturbance warning systems in the Amazon shows the potential of combined SAR-optical monitoring. Int. J. Remote Sens. 44, 59–77. https://doi.org/10.1080/01431161.2022.2157684.

Doblas, J., Reis, M.S., Belluzzo, A.P., Quadros, C.B., Moraes, D.R.V., Almeida, C.A., Maurano, L.E.P., Carvalho, A.F.A., Sant'Anna, S.J.S., Shimabukuro, Y.E., 2022. DETER-R: an operational near-real time tropical forest disturbance warning system based on Sentinel-1 time series analysis. Remote Sens. 14 https://doi.org/10.3390/rs14153658.

Drusch, M., Del Bello, U., Carlier, S., Colin, O., Fernandez, V., Gascon, F., Hoersch, B., Isola, C., Laberinti, P., Martimort, P., Meygret, A., Spoto, F., Sy, O., Marchese, F., Bargellini, P., 2012. Sentinel-2: ESA's optical high-resolution mission for GMES operational services. Remote Sens. Environ. 120, 25–36. https://doi.org/10.1016/j.rse.2011.11.026.

Dupuis, C., Fayolle, A., Bastin, J.F., Latte, N., Lejeune, P., 2023. Monitoring selective logging intensities in Central Africa with sentinel-1: a canopy disturbance experiment. Remote Sens. Environ. 298 https://doi.org/10.1016/j.rse.2023.113828.

Edwards, D.P., Tobias, J.A., Sheil, D., Meijaard, E., Laurance, W.F., 2014. Maintaining ecosystem function and services in logged tropical forests. Trends Ecol. Evol. https://doi.org/10.1016/j.tree.2014.07.003.

Ellis, P.W., Gopalakrishna, T., Goodman, R.C., Putz, F.E., Roopsind, A., Umunay, P.M., Zalman, J., Ellis, E.A., Mo, K., Gregoire, T.G., Griscom, B.W., 2019. Reduced-impact logging for climate change mitigation (RIL-C) can halve selective logging emissions from tropical forests. For. Ecol. Manag. 438, 255–266. https://doi.org/10.1016/j.foreco.2019.02.004.

Engert, J.E., Campbell, M.J., Cinner, J.E., Ishida, Y., Sloan, S., Supriatna, J., Alamgir, M., Cislowski, J., Laurance, W.F., 2024. Ghost roads and the destruction of Asia-Pacific tropical forests. Nature. https://doi.org/10.1038/s41586-024-07303-5.

European Space Agency, 2022. SNAP - ESA Sentinel Application Platform.

FAO, 2015. Global Administrative Unit Layers (GAUL).

Farr, T.G., Rosen, P.A., Caro, E., Crippen, R., Duren, R., Hensley, S., Kobrick, M., Paller, M., Rodriguez, E., Roth, L., Seal, D., Shaffer, S., Shimada, J., Umland, J., Werner, M., Oskin, M., Burbank, D., Alsdorf, D.E., 2007. The shuttle radar topography mission. Rev. Geophys. 45 https://doi.org/10.1029/2005RG000183.

Finer, B.M., Novoa, S., Weisse, M.J., Petersen, R., Mascaro, J., Souto, T., Stearns, F., Martinez, R.G., 2018. Combating deforestation: from satellite to intervention. Science 1979 (360), 1303–1305. https://doi.org/10.1126/science.aat1203.

Gaveau, D.L.A., Sloan, S., Molidena, E., Yaen, H., Sheil, D., Abram, N.K., Ancrenaz, M., Nasi, R., Quinones, M., Wielaard, N., Meijaard, E., 2014. Four decades of forest persistence, clearance and logging on Borneo. PLoS One 9. https://doi.org/10.1371/journal.pone.0101654.

Gaveau, D.L.A., Santos, L., Locatelli, B., Salim, M.A., Husnayaen, H., Meijaard, E., Heatubun, C., Sheil, D., 2021. Forest loss in Indonesian New Guinea (2001–2019): trends, drivers and outlook. Biol. Conserv. 261 https://doi.org/10.1016/j.biocon.2021.109225.

Gibson, L., Lee, T.M., Koh, L.P., Brook, B.W., Gardner, T.A., Barlow, J., Peres, C.A., Bradshaw, C.J.A., Laurance, W.F., Lovejoy, T.E., Sodhi, N.S., 2011. Primary forests are irreplaceable for sustaining tropical biodiversity. Nature 478, 378–381. https://doi.org/10.1038/nature10425.

Gideon Neba, S., Kanninen, M., Eba'a Atyi, R., Sonwa, D.J., 2014. Assessment and prediction of above-ground biomass in selectively logged forest concessions using field measurements and remote sensing data: case study in South East Cameroon. For. Ecol. Manag. 329, 177–185. https://doi.org/10.1016/j.foreco.2014.06.018.

Global Forest Watch, 2024. Managed Forest Concessions, Accessed Through Global Forest Watch. www.globalforestwatch.org.

Gorelick, N., Hancher, M., Dixon, M., Ilyushchenko, S., Thau, D., Moore, R., 2017. Google Earth Engine: planetary-scale geospatial analysis for everyone. Remote Sens. Environ. 202, 18–27. https://doi.org/10.1016/j.rse.2017.06.031.

Gou, Y., Balling, J., De Sy, V., Herold, M., De Keersmaecker, W., Slagter, B., Mullissa, A., Shang, X., Reiche, J., 2022. Intra-annual relationship between precipitation and forest disturbance in the African rainforest. Environ. Res. Lett. 17, 044044 https://doi.org/10.1088/1748-9326/ac5ca0.

Hansen, M.C., Potapov, P.V., Moore, R., Hancher, M., Turubanova, S.A., Tyukavina, A., Thau, D., Stehman, S.V., Goetz, S.J., Loveland, T.R., Kommareddy, A., Egorov, A., Chini, L., Justice, C.O., Townshend, J.R.G., 2013. High-resolution global maps of 21st-century forest cover change. Science 1979, 342. https://doi.org/10.1126/science.1244693.

Hansen, M.C., Krylov, A., Tyukavina, A., Potapov, P.V., Turubanova, S., Zutta, B., Ifo, S., Margono, B., Stolle, F., Moore, R., 2016. Humid tropical forest disturbance alerts using Landsat data. Environ. Res. Lett. 11 https://doi.org/10.1088/1748-9326/11/3/034008.

Hethcoat, M.G., Carreiras, J.M.B., Edwards, D.P., Bryant, R.G., Quegan, S., 2021. Detecting tropical selective logging with C-band SAR data may require a time series approach. Remote Sens. Environ. 259 https://doi.org/10.1016/j.rse.2021.112411.

Hoekman, D., Kooij, B., Quiñones, M., Vellekoop, S., Carolita, I., Budhiman, S., Arief, R., Roswintiarti, O., 2020. Wide-area near-real-time monitoring of tropical forest degradation and deforestation using Sentinel-1. Remote Sens. 12, 1–32. https://doi.org/10.3390/rs12193263.

Ibisch, P.L., Hoffmann, M.T., Kreft, S., Pe'Er, G., Kati, V., Biber-Freudenberger, L., DellaSala, D.A., Vale, M.M., Hobson, P.R., Selva, N., 2016. A global map of roadless areas and their conservation status. Science 1979, 354. https://doi.org/10.1126/science.aaf7166.

UNEP-WCMC and IUCN, 2022. Protected Planet: The World Database on Protected Areas (WDPA). www.protectedplanet.net.

Joshi, N., Baumann, M., Ehammer, A., Fensholt, R., Grogan, K., Hostert, P., Jepsen, M.R., Kuemmerle, T., Meyfroidt, P., Mitchard, E.T.A., Reiche, J., Ryan, C.M., Waske, B., 2016. A review of the application of optical and radar remote sensing data fusion to land use mapping and monitoring. Remote Sens. https://doi.org/10.3390/rs8010070.

Kingma, D.P., Ba, J.L., 2015. Adam: A method for stochastic optimization. In: 3rd International Conference on Learning Representations, ICLR 2015 - Conference Track Proceedings.

Kleinschroth, F., Healey, J.R., 2017. Impacts of logging roads on tropical forests. Biotropica. https://doi.org/10.1111/btp.12462.

Kleinschroth, F., Gourlet-Fleury, S., Sist, P., Mortier, F., Healey, J.R., 2015. Legacy of logging roads in the Congo Basin: how persistent are the scars in forest cover? Ecosphere 6. https://doi.org/10.1890/ES14-00488.1.

Kleinschroth, F., Healey, J.R., Sist, P., Mortier, F., Gourlet-Fleury, S., 2016. How persistent are the impacts of logging roads on central African forest vegetation? J. Appl. Ecol. 53, 1127–1137. https://doi.org/10.1111/1365-2664.12661.

Kleinschroth, F., Garcia, C., Ghazoul, J., 2019a. Reconciling certification and intact forest landscape conservation. Ambio 48, 153–159. https://doi.org/10.1007/s13280-018-1063-6.

Kleinschroth, F., Laporte, N., Laurance, W.F., Goetz, S.J., Ghazoul, J., 2019b. Road expansion and persistence in forests of the Congo Basin. Nat. Sustain. 2, 628–634. https://doi.org/10.1038/s41893-019-0310-6.

Kleinschroth, F., Rayden, T., Ghazoul, J., 2019c. The dilemma of maintaining intact Forest through certification. Front. For. Glob. Chang. 2 https://doi.org/10.3389/ffgc.2019.00072.

Laporte, N.T., Stabach, J.A., Grosch, R., Lin, T.S., Goetz, S.J., 2007. Expansion of industrial logging in Central Africa. Science (1979) 316, 1451. https://doi.org/10.1126/science.1141057.

Laurance, W.F., Goosem, M., Laurance, S.G.W., 2009. Impacts of roads and linear clearings on tropical forests. Trends Ecol. Evol. https://doi.org/10.1016/j.tree.2009.06.009.

Laurance, W.F., Clements, G.R., Sloan, S., O'Connell, C.S., Mueller, N.D., Goosem, M., Venter, O., Edwards, D.P., Phalan, B., Balmford, A., Van Der Ree, R., Arrea, I.B., 2014. A global strategy for road building. Nature 513, 229–232. https://doi.org/10.1038/nature13717.

Lian, R., Wang, W., Mustafa, N., Huang, L., 2020. Road extraction methods in high-resolution remote sensing images: a comprehensive review. IEEE J. Sel. Top. Appl. Earth Obs. Remote Sens. https://doi.org/10.1109/JSTARS.2020.3023549.

Lima, T.A., Beuchle, R., Langner, A., Grecchi, R.C., Griess, V.C., Achard, F., 2019. Comparing Sentinel-2 MSI and Landsat 8 OLI imagery for monitoring selective logging in the Brazilian Amazon. Remote Sens. 11 https://doi.org/10.3390/rs11080922.

Lynch, J., Maslin, M., Balzter, H., Sweeting, M., 2013. Choose satellites to monitor deforestation. Nature 496, 293–294.

Mermoz, S., Bouvet, A., Koleck, T., Ballère, M., Le Toan, T., 2021. Continuous detection of forest loss in Vietnam, Laos, and Cambodia using Sentinel-1 data. Remote Sens. 13 https://doi.org/10.3390/rs13234877.

Nyberg, B., Henstra, G., Gawthorpe, R.L., Ravnås, R., Ahokas, J., 2023. Global scale analysis on the extent of river channel belts. Nat. Commun. 14 https://doi.org/10.1038/s41467-023-37852-8.

OpenStreetMap contributors, 2024. Forestry Tracks. https://www.openstreetmap.org/.

Pearson, T.R.H., Brown, S., Casarim, F.M., 2014. Carbon emissions from tropical forest degradation caused by logging. Environ. Res. Lett. 9 https://doi.org/10.1088/1748-9326/9/3/034017.

Pekel, J.F., Cottam, A., Gorelick, N., Belward, A.S., 2016. High-resolution mapping of global surface water and its long-term changes. Nature 540. https://doi.org/10.1038/nature20584.

Philippon, N., Cornu, G., Monteil, L., Gond, V., Moron, V., Pergaud, J., Sèze, G., Bigot, S., Camberlin, P., Doumenge, C., Fayolle, A., Ngomanda, A., 2019. The light-deficient

climates of western Central African evergreen forests. Environ. Res. Lett. 14 https://doi.org/10.1088/1748-9326/aaf5d8.

Pickens, A.H., Hansen, M.C., Adusei, B., Potapov, P., 2020a. Sentinel-2 Forest Loss Alert. Global Land Analysis and Discovery (GLAD).

Pickens, A.H., Hansen, M.C., Hancher, M., Stehman, S.V., Tyukavina, A., Potapov, P., Marroquin, B., Sherani, Z., 2020b. Mapping and sampling to characterize global inland water dynamics from 1999 to 2018 with full Landsat time-series. Remote Sens. Environ. 243 https://doi.org/10.1016/j.rse.2020.111792.

Planet Team, 2017. Planet Application Program Interface: In Space for Life on Earth.

Potapov, P., Yaroshenko, A., Turubanova, S., Dubinin, M., Laestadius, L., Thies, C., Aksenov, D., Egorov, A., Yesipova, Y., Glushkov, I., Karpachevskiy, M., Kostikova, A., Manisha, A., Tsybikova, E., Zhuravleva, I., 2008. Mapping the world's intact forest landscapes by remote sensing. Ecol. Soc. 13 https://doi.org/10.5751/ES-02670-130251.

Potapov, P., Hansen, M.C., Laestadius, L., Turubanova, S., Yaroshenko, A., Thies, C., Smith, W., Zhuravleva, I., Komarova, A., Minnemeyer, S., Esipova, E., 2017. The last frontiers of wilderness: tracking loss of intact forest landscapes from 2000 to 2013. Sci. Adv. 3 https://doi.org/10.1126/sciadv.1600821.

Putz, F.E., Pinard, M.A., 1993. Reduced-impact logging as a carbon-offset method. Conserv. Biol. 7 https://doi.org/10.1046/j.1523-1739.1993.7407551.x.

Putz, F.E., Zuidema, P.A., Synnott, T., Peña-Claros, M., Pinard, M.A., Sheil, D., Vanclay, J.K., Sist, P., Gourlet-Fleury, S., Griscom, B., Palmer, J., Zagt, R., 2012. Sustaining conservation values in selectively logged tropical forests: the attained and the attainable. Conserv. Lett. 5 https://doi.org/10.1111/j.1755-263X.2012.00242.x.

Reiche, J., Lucas, R., Mitchell, A.L., Verbesselt, J., Hoekman, D.H., Haarpaintner, J., Kellndorfer, J.M., Rosenqvist, A., Lehmann, E.A., Woodcock, C.E., Seifert, F.M., Herold, M., 2016. Combining satellite data for better tropical forest monitoring. Nat. Clim. Chang. https://doi.org/10.1038/nclimate2919.

Reiche, J., Mullissa, A., Slagter, B., Gou, Y., Tsendbazar, N.E., Odongo-Braun, C., Vollrath, A., Weisse, M.J., Stolle, F., Pickens, A., Donchyts, G., Clinton, N., Gorelick, N., Herold, M., 2021. Forest disturbance alerts for the Congo Basin using Sentinel-1. Environ. Res. Lett. 16 https://doi.org/10.1088/1748-9326/abd0a8.

Reiche, J., Balling, J., Pickens, A.H., Masolele, R.N., Berger, A., Weisse, M.J., Mannarino, D., Gou, Y., Slagter, B., Donchyts, G., Carter, S., 2024. Integrating satellite-based forest disturbance alerts improves detection timeliness and confidence. Environ. Res. Lett. 19 https://doi.org/10.1088/1748-9326/ad2d82.

Riggio, J., Baillie, J.E.M., Brumby, S., Ellis, E., Kennedy, C.M., Oakleaf, J.R., Tait, A., Tepe, T., Theobald, D.M., Venter, O., Watson, J.E.M., Jacobson, A.P., 2020. Global human influence maps reveal clear opportunities in conserving Earth's remaining intact terrestrial ecosystems. Glob. Chang. Biol. 26 https://doi.org/10.1111/gcb.15109.

Ronneberger, O., Fischer, P., Brox, T., 2015. U-net: Convolutional networks for biomedical image segmentation. In: International Conference on Medical Image Computing and Computer-Assisted Intervention. https://doi.org/10.1007/978-3-319-24574-4_28.

Shapiro, A., d'Annunzio, R., Desclée, B., Jungers, Q., Kondjo, H.K., Iyanga, J.M., Gangyo, F.I., Nana, T., Obame, C.V., Milandou, C., Rambaud, P., Sonwa, D.J., Mertens, B., Tchana, E., Khasa, D., Bourgoin, C., Ouissika, C.B., Kipute, D.D., 2023. Small scale agriculture continues to drive deforestation and degradation in fragmented forests in the Congo Basin (2015–2020). Land Use Policy 134. https://doi.org/10.1016/j.landusepol.2023.106922.

Slagter, B., Reiche, J., Marcos, D., Mullissa, A., Lossou, E., Peña-Claros, M., Herold, M., 2023. Monitoring direct drivers of small-scale tropical forest disturbance in near real-time with Sentinel-1 and -2 data. Remote Sens. Environ. 295 https://doi.org/10.1016/j.rse.2023.113655.

Sloan, S., Campbell, M.J., Alamgir, M., Collier-Baker, E., Nowak, M.G., Usher, G., Laurance, W.F., 2018. Infrastructure development and contested forest governance threaten the Leuser Ecosystem, Indonesia. Land Use Policy 77. https://doi.org/10.1016/j.landusepol.2018.05.043.

Sloan, S., Talkhani, R.R., Huang, T., Engert, J., Laurance, W.F., 2024. Mapping remote roads using artificial intelligence and satellite imagery. Remote Sens. 16, 839. https://doi.org/10.3390/rs16050839.

Sudre, C.H., Li, W., Vercauteren, T., Ourselin, S., Jorge Cardoso, M., 2017. Generalised dice overlap as a deep learning loss function for highly unbalanced segmentations. In: Lecture Notes in Computer Science (Including Subseries Lecture Notes in Artificial Intelligence and Lecture Notes in Bioinformatics). https://doi.org/10.1007/978-3-319-67558-9_28.

Tanase, M.A., Aponte, C., Mermoz, S., Bouvet, A., Le Toan, T., Heurich, M., 2018. Detection of windthrows and insect outbreaks by L-band SAR: a case study in the Bavarian Forest National Park. Remote Sens. Environ. 209 https://doi.org/10.1016/j.rse.2018.03.009.

Torres, R., Snoeij, P., Geudtner, D., Bibby, D., Davidson, M., Attema, E., Potin, P., Rommen, B.Ö., Floury, N., Brown, M., Traver, I.N., Deghaye, P., Duesmann, B., Rosich, B., Miranda, N., Bruno, C., L'Abbate, M., Croci, R., Pietropaolo, A., Huchler, M., Rostan, F., 2012. GMES Sentinel-1 mission. Remote Sens. Environ. 120 https://doi.org/10.1016/j.rse.2011.05.028.

Touzi, R., Sasitiwarih, A., 2001. RADARSAT optimum configurations for trail and road detection in indonesian forests. Can. J. Remote. Sens. 27, 555–567. https://doi.org/10.1080/07038992.2001.10854895.

Turubanova, S., Potapov, P.V., Tyukavina, A., Hansen, M.C., 2018. Ongoing primary forest loss in Brazil, Democratic Republic of the Congo, and Indonesia. Environ. Res. Lett. 13 https://doi.org/10.1088/1748-9326/aacd1c.

Umunay, P.M., Gregoire, T.G., Gopalakrishna, T., Ellis, P.W., Putz, F.E., 2019. Selective logging emissions and potential emission reductions from reduced-impact logging in the Congo Basin. For. Ecol. Manag. 437, 360–371. https://doi.org/10.1016/j.foreco.2019.01.049.

Vancutsem, C., Achard, F., Pekel, J.-F., Vieilledent, G., Carboni, S., Simonetti, D., Gallego, J., Aragão, L.E.O.C., Nasi, R., 2021. Long-term (1990-2019) monitoring of forest cover changes in the humid tropics. Sci. Adv. 7 https://doi.org/10.1126/sciadv.abe1603.

Vargas, C., Montalban, J., Leon, A.A., 2019. Early warning tropical forest loss alerts in Peru using landsat. Environ. Res. Commun. https://doi.org/10.1088/2515-7620/ab4ec3.

Venter, O., Sanderson, E.W., Magrach, A., Allan, J.R., Beher, J., Jones, K.R., Possingham, H.P., Laurance, W.F., Wood, P., Fekete, B.M., Levy, M.A., Watson, J.E.M., 2016. Sixteen years of change in the global terrestrial human footprint and implications for biodiversity conservation. Nat. Commun. 7 https://doi.org/10.1038/ncomms12558.

Watanabe, M., Koyama, C.N., Hayashi, M., Nagatani, I., Tadono, T., Shimada, M., 2021. Refined algorithm for forest early warning system with ALOS-2/PALSAR-2 ScanSAR data in tropical forest regions. Remote Sens. Environ. 265, 112643 https://doi.org/10.1016/j.rse.2021.112643.

Weisse, M.J., Noguerón, R., Eduardo, R., Vicencio, V., Arturo, D., Soto, C., 2019. Use of Near-Real-Time Deforestation Alerts: A Case Study from Peru.

Welsink, A.J., Reiche, J., de Sy, V., Carter, S., Slagter, B., Suarez, D.R., Batros, B., Peña-Claros, M., Herold, M., 2023. Towards the use of satellite-based tropical forest disturbance alerts to assess selective logging intensities. Environ. Res. Lett. 18 https://doi.org/10.1088/1748-9326/acd018.

WWF, 2022. One step ahead in preventing illegal deforestation.

Zupanc, A, 2017. Improving Cloud Detection with Machine Learning. https://medium.com/sentinel-hub/improving-cloud-detection-with-machine-learning-c09dc5d7cf13.

Zwerts, J.A., van der Linde, C.M., Praamstra, G.J., Schipper, J., Trolliet, F., Waeber, P.O., Garcia, C.A., 2024. Feasibility and effectiveness of global intact forest landscape protection through forest certification: the conservation burden of intact forest landscapes. Frontiers in Forests and Global Change 7. https://doi.org/10.3389/ffgc.2024.1335430.